Unified approach to some transport and EPR properties of noble metals with rare-earth impurities*

G. Lacueva and P. M. Levy
Department of Physics, New York University, 4 Washington Place, New York, New York 10003

A. Fert
Laboratoire de Physique des Solides, Universite de Paris-Sud, 91405 Orsay, France
(Received 20 January 1982)

Both magnetotransport and EPR experiments have shown the importance of the anisotropic character of the k-f interaction between conduction and $4f$ electrons. For noble metals with rare-earth impurities the magnitude of the anisotropic terms can be understood in terms of the hybridization of the conduction electrons with the outer $5d$ electrons of the rare-earth impurities. To obtain a consistent description of the magnetotransport properties we have included the spin-orbit coupling of the $5d$ electrons as well as their crystal-field splitting. The various parameters entering our model have been determined by fitting the isotropic transport properties as well as the anisotropic magnetoresistance arising from quadrupole scattering and the Hall effect due to skew scattering. We have used this model to calculate the $5d$ virtual bound state contribution to the g shift and linewidth of rare-earth impurities in noble metals. After estimating the s contribution we obtain a consistent fit for the g shift and linewidth of several rare earths in noble metals.

I. INTRODUCTION

The conduction-electron—local-moment (k-f) interaction plays a central role in the understanding of the magnetic properties of alloys and compounds. Early attempts to describe the effects of k-f scattering were based on the isotropic exchange interaction $J\vec{s}\cdot\vec{S}$. However, this approach cannot explain the anisotropic transport effects (anisotropy of resistivity and extraordinary Hall effect) and also in many systems cannot account for other properties such as the EPR g shift and linewidth. Huang-Liu, Ling, and Orbach[1] and Fert and Levy[2] have proposed a model for the k-f interaction based on a virtual bound state (VBS) description for the rare earths's outer $5d$ electrons and on taking into account all the components of the $4f$-$5d$ Coulomb interaction, i.e., orbital and multipole terms as well as the isotropic spin interaction. Conduction electrons in virtual-bound states sense the highly anisotropic $4f$ charge density because the $5d$ electrons's radial wave function is much closer to the $4f$ electrons than the diffuse spherical Bessel functions which are the radial wave functions for conduction electrons in plane-wave states. This model gave the correct order of magnitudes for much of the magnetotransport and electron paramagnetic resonance (EPR) data; however, some shortcomings were evident. First, while one could explain the orbital contribution of the extraordinary Hall effect, the large spin contribution as evidenced for gadolinium impurities in metals is not accounted for, and second, by using phase shifts η determined from the fits to magnetotransport data, one obtained g shift and linewidth extremely different from those observed.

To remedy these discrepancies it was noted that the spin-orbit coupling of the conduction electrons had to be taken into account. Fert and Friederich considered the role of spin-orbit coupling in producing skew scattering of conduction electrons by local moments,[3] and Orbach and Huang-Liu showed that the introduction of spin-orbit coupling might improve the agreement with EPR experiments.[4]

We have extended the VBS picture of the k-f interaction by (i) including the spin-orbit coupling of the conduction electrons, which we study in two limiting cases, the free $5d$ VBS and the cubic crystal-field split $5d$-t_{2g} VBS, (ii) including the p character of the conduction electrons (η_1 phase shifts) in our calculation of the transport proper-

ties, and (iii) calculating when necessary the T matrix to second order in the distorted-wave Born approximation.

Specifically, we considered the following transport data for silver and gold with rare-earth impurities, the residual resistivity ρ_0 due to the spherical scattering of the conduction electrons by the impurities, the thermoelectric power S/T, the isotropic and anisotropic magnetoresistance, and the extraordinary contribution to the Hall resistivity. We have calculated these properties based on the above model of the k-f scattering and fit the phase shifts η_l and the $5d$-$4f$ interaction parameters A_k to obtain the best fit to the data. We were able to obtain reasonable fits to the data with both the free $5d$ VBS and the cubic crystal-field split $5d$-t_{2g} VBS. Of the two models, the t_{2g} is the preferred one because the effective spin-orbit coupling parameter λ is much closer to its atomic value.

To check the validity of the parameters (η_l,λ,A_k) we found in our fits to the transport data, we recalculated on the basis of the same model the contribution from the d wave scattering to the g shift Δg and linewidth ΔH of the rare-earth resonance in silver and gold. Only the model with the $5d$-t_{2g} VBS gave acceptable values; the free-$5d$ VBS model gave $5d$ contributions to Δg and ΔH which were much smaller than the experimental values. The most encouraging result of our study has been that we were able to fit the resonance data on rare-earth impurities in silver and gold by using the parameters determined from our analysis of transport measurements.

In Sec. II we derive the scattering matrix elements due to the k-f interaction on the basis of a $5d$ VBS with spin-orbit coupling for the crystal-field split t_{2g} ground state. We have carried out our calculations to second order in the distorted-wave Born approximation in order to include effects such as the anisotropy of the magnetoresistivity of Gd^{3+} (an S-state ion) which comes from the spin-orbit coupling of the $5d$ electron. Our matrix elements are expressed in terms of the conduction-electron phase shifts η_l, their spin-orbit coupling λ, and the $5d$-$4f$ interaction parameters A_k. In the next section we use these scattering matrix elements to calculate the transport and resonance properties of interest in terms of the above parameters for the case of a $5d$-t_{2g} VBS. In the Appendix we consider the case of the full $5d$ VBS (without a crystal-field splitting). Comparisons between experiments and theory are made in Sec. IV and in the concluding section we summarize our findings.

II. DERIVATION OF THE SCATTERING MATRIX ELEMENTS

The scattering potential V can be written as the sum of two terms,

$$V=V_0+v \tag{2.1}$$

where V_0 is a spherical term which takes into account the attraction of about two electrons (mostly in $5d$ and $6s$ states) and v is the Coulomb interaction, direct and exchange, of the conduction electron with the $4f$ electrons that depends on the orientation of the $4f$ moment. Since V_0 is 1 order of magnitude larger than v and is comparable to the conduction-electron energy, we cannot treat it in the Born approximation. Rather, one first takes V_0 into account to modify the wave functions in the vicinity of the impurity and obtains an expression for the perturbation in terms of phase shifts. Then the contribution to the T matrix from v is calculated by using these phase-shifted wave functions and the Born approximation, i.e., the distorted-wave Born approximation.

The matrix elements of the T matrix for the system we are studying can be written as[5]

$$T_{\vec{k}\sigma,\vec{k}'\sigma'}=T^{(0)}_{\vec{k}\sigma,\vec{k}'\sigma'}+\langle \vec{k}'^{(-)}\sigma' \mid v \mid \psi^{\pm}_{\vec{k}\sigma}\rangle \ , \tag{2.2}$$

where $T^{(0)}$ is the T matrix for a system in which V_0 is the full potential, $|k'^{(-)}\sigma'\rangle$ is an incoming wave for the scattering in the potential V_0 alone, and $|\psi^{\pm}_{\vec{k}\sigma}\rangle$ is the scattered wave function in the presence of V_0 and v.

Since $|\psi^{\pm}_{\vec{k}\sigma}\rangle$ is written as

$$|\psi^{(+)}_{\vec{k}\sigma}\rangle=|\vec{k}^{(+)}\sigma\rangle+\frac{1}{\epsilon_k-H_0-V_0+i\eta}v\,|\psi^{(+)}_{\vec{k}\sigma}\rangle \ ,$$

we can approximate it to second order by[5]

$$\begin{aligned}|\psi^{(+)}_{\vec{k}\sigma}\rangle &\simeq |\vec{k}^{(+)}\sigma\rangle+\frac{1}{(\epsilon_k-H_0-V_0+i\eta)}v\,|\vec{k}^{(+)}\sigma\rangle \\ &=|\vec{k}^{(+)}\sigma\rangle+Gv\,|\vec{k}^{(+)}\sigma\rangle \ ,\end{aligned} \tag{2.3}$$

where G is the Green's function for the scattering in presence of V_0 only.

We can write the T matrix elements as:

$$\begin{aligned}T_{\vec{k}\sigma,\vec{k}'\sigma'}=&T^{(0)}_{\vec{k}\sigma,\vec{k}'\sigma'}+dT^{(1)}_{\vec{k}\sigma,\vec{k}'\sigma'} \\ &+dT^{(2)}_{\vec{k}\sigma,\vec{k}'\sigma'}+\cdots \ ,\end{aligned} \tag{2.4}$$

where

$$T^{(0)}_{\vec{k}\sigma,\vec{k}'\sigma'}=\langle \vec{k}'\sigma' \mid V_0 \mid \vec{k}^{(+)}\sigma\rangle \ , \tag{2.5}$$

$$dT^{(1)}_{\vec{k}\sigma,\vec{k}'\sigma'}=\langle \vec{k}'^{(-)}\sigma' \mid v \mid \vec{k}^{(+)}\sigma\rangle \ , \tag{2.6}$$

$$dT^{(2)}_{\vec{k}\sigma,\vec{k}'\sigma'}=\langle \vec{k}'^{(-)}\sigma' \mid vGv \mid \vec{k}^{(+)}\sigma\rangle \ , \tag{2.7}$$

and $\langle \vec{k}'\sigma' \mid$ is the unperturbed plane-wave state. The transition probability $W_{\vec{k}\sigma,\vec{k}'\sigma'}$ is related to the T matrix by

$$W_{\vec{k}\sigma,\vec{k}'\sigma'}=\frac{2\pi}{\hbar}\mid T^{(0)}_{\vec{k}\sigma,\vec{k}'\sigma'}+dT^{(1)}_{\vec{k}\sigma,\vec{k}'\sigma'}+dT^{(2)}_{\vec{k}\sigma,\vec{k}'\sigma'}+\cdots\mid^2\delta(\epsilon_k-\epsilon_{k'}) \ .$$

To second order in the perturbation v, the transition probability is given as

$$W_{\vec{k}\sigma,\vec{k}'\sigma'}\simeq\frac{2\pi}{\hbar}[\mid T^{(0)}_{\vec{k}\sigma,\vec{k}'\sigma'}\mid^2+(T^{(0)*}_{\vec{k}\sigma,\vec{k}'\sigma'}dT^{(1)}_{\vec{k}\sigma,\vec{k}'\sigma'}+\text{c.c.})$$
$$+\mid dT^{(1)}_{\vec{k}\sigma,\vec{k}'\sigma'}\mid^2+(T^{(0)*}_{\vec{k}\sigma,\vec{k}'\sigma'}dT^{(2)}_{\vec{k}\sigma,\vec{k}'\sigma'}+\text{c.c.})]\delta(\epsilon_k-\epsilon_{k'}) \ . \tag{2.8}$$

The wave function $\mid \vec{k}^{(\pm)}\sigma\rangle$ for a spin-orbit split t_{2g} state can be written, according to Friedel's theory of nonmagnetic virtual bound states,[6] as

$$\mid \vec{k}^{(\pm)}\sigma\rangle=\sum_{\alpha j}C^{\pm}_{\alpha j}(\vec{k})\mid jm_j\rangle+\cdots \ . \tag{2.9}$$

Only the part corresponding to the admixture of local d states has been written and

$$C^{\pm}_{\alpha j}(\vec{k})=e^{\pm i\eta_j}\sin\eta_j\frac{\langle d\mid V_0\mid k\rangle}{\Delta}Y_\alpha(\Omega_{\vec{k}})\langle jm_j\mid\alpha\sigma\rangle \ ,$$

where $\langle jm_j\mid\alpha\sigma\rangle$ is a transformation matrix element (Clebsch-Gordan coefficient) from the uncoupled basis to a spin-orbit coupled one and Δ is the half-width of the VBS. The phase shift η_j is given by

$$\eta_j=\tan^{-1}\frac{\Delta}{\epsilon_{rj}-\epsilon(k)} \ , \tag{2.10}$$

where ϵ_{rj} is the energy of the center of the VBS resonance. The matrix element $\langle d\mid V_0\mid k\rangle$, which represents the mixing of d and conduction electrons, is related to Δ by

$$\mid\langle d\mid V_0\mid k\rangle\mid^2=\frac{4\Delta}{N(E_F)} \ , \tag{2.11}$$

where $N(E_F)$ is the density of states per unit volume per one spin direction at the Fermi level, and $Y_\alpha(\Omega_{\vec{k}})$ are Kubic harmonics.[7]

The admixture of $5d$ states into the conduction-electron wave function gives the main contribution to the matrix elements of v between $\mid \vec{k}^{(\pm)}\sigma\rangle$ states so that these matrix elements can be written in terms of the elements of the $4f$-$5d$ interaction. Writing this interaction in tensorial notation we have, for one $4f$ electron,

$$H=\sum_k F^k(3\mid\mid C^k\mid\mid 3)(2\mid\mid C^k\mid\mid 2)u_f^{(k)}\cdot u_d^{(k)}$$
$$+\sum_{r,k}(-1)^{r+k}(2k+1)G^r(2\mid\mid C^r\mid\mid 3)^2\begin{Bmatrix}3&3&k\\2&2&r\end{Bmatrix}[\tfrac{1}{2}u_f^{(k)}\cdot u_d^{(k)}+2(\vec{s}_f\cdot\vec{s}_d)(u_f^{(k)}\cdot u_d^{(k)})] \ , \tag{2.12}$$

where F^k and G^k are the direct and exchange Slater integrals; the tensor operators $u^{(k)}$ are defined by

$$(nl\mid\mid u^{(k)}\mid\mid n'l')=\delta_{nn'}\delta_{ll'} \ , \tag{2.13}$$

and the reduced matrix elements of the spherical harmonics are defined as

$$(l\mid\mid C^k\mid\mid l')=(-1)^l[(2l+1)(2l'+1)]^{1/2}\begin{Bmatrix}l&k&l'\\0&0&0\end{Bmatrix} \ ,$$

where the large parentheses denote a $3-j$ symbol and the curly bracket in Eq. (2.12) a $6-j$ symbol.

To obtain the interaction for n $4f$ electrons one replaces s_f and $u_f^{(k)}$ by sums over all the $4f$ electrons. From the Hamiltonian Eq. (2.12) we find for v the following expression:

$$v=-\mathscr{P}_0A_0\vec{s}\cdot\vec{J}-\mathscr{P}_1A_1\vec{l}\cdot\vec{J}+15\sqrt{7}\mathscr{P}_2A_2(s^1\times u^2)^1_d\cdot\vec{J}+3\sqrt{35/2}\mathscr{P}_3A_3u_d^2\cdot O^2(J)$$
$$-6\sqrt{5}\mathscr{P}_4A_4(s^1\times u^1)^2_d\cdot O^2(J)-7\sqrt{10/3}\mathscr{P}_5A_5(s^1\times u^3)^2_d\cdot O^2(J)+\cdots \ , \tag{2.14}$$

where $\vec{J}$ is the total angular momentum of the $4f$ shell, and

$$\mathscr{P}_0=(g_J-1)\ ,$$

$$\mathscr{P}_1=(2-g_J)\ ,$$

$$\mathscr{P}_2=\frac{\left\langle J\left|\left|\sum_i (s^1\times u^2)^1(i)\right|\right|J\right\rangle}{(J||J||J)}\ ,$$

$$\mathscr{P}_3=\frac{\left\langle J\left|\left|\sum_i u^2(i)\right|\right|J\right\rangle}{(J||O^2||J)}\ ,$$

$$\mathscr{P}_4=\frac{\left\langle J\left|\left|\sum_i (s^1\times u^1)^2(i)\right|\right|J\right\rangle}{(J||O^2||J)}\ ,$$

$$\mathscr{P}_5=\frac{\left\langle J\left|\left|\sum_i (s^1\times u^3)^2(i)\right|\right|J\right\rangle}{(J||O^2||J)}\ .$$

The sums are over the $4f$ electrons; the values of these coefficients are given in Table I. Finally,

$$A_0=\tfrac{2}{35}(3G^1+\tfrac{4}{3}G^3+\tfrac{50}{33}G^5)\ ,$$

$$A_1=\tfrac{1}{280}(4G^1+\tfrac{2}{3}G^3-\tfrac{50}{33}G^5)\ ,$$

$$A_2=\tfrac{4}{2205}(9G^1-\tfrac{11}{6}G^3+\tfrac{125}{66}G^5)\ ,$$

$$A_3=\frac{2}{3\sqrt{105}}(2F^2-\tfrac{9}{7}G^1+\tfrac{11}{42}G^3-\tfrac{125}{462}G^5)\ ,$$

$$A_4=\frac{1}{5\sqrt{14}}(4G^1+\tfrac{2}{3}G^5-\tfrac{50}{33}G^5)\ ,$$

$$A_5=\frac{\sqrt{2}}{105}(27G^1-8G^3-\tfrac{25}{11}G^5)\ ,$$

where F^k and G^k are the Slater direct and exchange integrals. By using Eq. (2.9) in Eqs. (2.5)–(2.7), we obtain for the T matrix elements

$$T^{(0)}_{\vec{k}\sigma,\vec{k}'\sigma'}=\frac{-4}{N(E_F)}\left[\frac{\delta\sigma\sigma'}{4\pi}e^{i\eta_0}\sin\eta_0+\delta\sigma\sigma' e^{i\eta_1}\sin\eta_1\sum_m Y^*_{1m}(\Omega_{\vec{k}})Y_{1m}(\Omega_{\vec{k}'})\right.$$
$$\left.+\sum_j e^{\eta_j}\sin\eta_j\sum_{\substack{m_1\\m_2}}{}'\langle m_2\sigma'\,|\,jm_j\rangle\langle jm_j\,|\,m_1\sigma\rangle Y_{m1}(\Omega_{\vec{k}})Y_{m2}(\Omega_{\vec{k}'})\right]\ . \tag{2.15}$$

The prime on the sum over m_1 and m_2 indicates the restriction

$$m_j=m_1+\sigma=m_2+\sigma'\ .$$

The matrix elements of the perturbation v are

$$dT^{(1)}_{\vec{k}\sigma,\vec{k}'\sigma'}=\frac{4}{N(E_F)\Delta}\sum_{jj'}\sum_{\substack{m_3\\m_4}}{}'\exp[i(\eta_j+\eta_{j'})]\sin\eta_j\sin\eta_{j'}\langle m_4\sigma'\,|\,j'm_{j'}\rangle\langle j'm_{j'}\,|\,v\,|\,jm_j\rangle$$
$$\times\langle jm_j\,|\,m_3\sigma\rangle Y^*_{m_4}(\Omega_{\vec{k}'})Y_{m_3}(\Omega_{\vec{k}})\ , \tag{2.16}$$

TABLE I. The coefficients $\mathscr{P}_k$ entering in the $4f$-$5d$ interaction [Eq. (2.14)].

	Gd	Tb	Dy	Ho	Er	Tm	Yb
$\mathscr{P}_0$	1	$\frac{1}{2}$	$\frac{1}{3}$	$\frac{1}{4}$	$\frac{1}{5}$	$\frac{1}{6}$	$\frac{1}{7}$
$\mathscr{P}_1$	0	$\frac{1}{2}$	$\frac{2}{3}$	$\frac{3}{4}$	$\frac{4}{5}$	$\frac{5}{6}$	$\frac{6}{7}$
$\mathscr{P}_2$	0	$-\frac{1}{12}$	$-\frac{1}{15}$	$-\frac{1}{40}$	$\frac{2}{75}$	$\frac{1}{12}$	$\frac{1}{7}$
$\mathscr{P}_3\times10^3$	0	9.06	5.7	2	−2.28	−9.05	−28.4
$\mathscr{P}_4\times10^3$	0	−4.95	−5.17	−5.45	−6.25	−8.27	−15.5
$\mathscr{P}_5\times10^3$	0	1.88	0	−1.03	−1.18	0	5.87

where

$$m_j = m_3 + \sigma \ ,$$

$$m_{j'} = m_4 + \sigma' \ ,$$

and v is given by Eq. (2.14).

For the $dT^{(2)}$ matrix element we have to take into account the noncommutativity of the operators present in v. This noncommutativity gives rise, for example, to the Kondo effect. We have

$$dT^{(2)}_{\vec{k}\sigma,\vec{k}'\sigma'} = \sum_{k''\sigma''} \frac{1}{(\epsilon_k - \epsilon_{k''} + i\mu)} (V_{\vec{k}'\sigma',\vec{k}''\sigma''} V_{\vec{k}''\sigma'',\vec{k}\sigma} - f_{k''\sigma''}[V_{\vec{k}'\sigma',\vec{k}''\sigma''}, V_{\vec{k}''\sigma'',\vec{k}\sigma}]), \tag{2.17}$$

where

$$V_{\vec{k}'\sigma',\vec{k}''\sigma''} = \langle \vec{k}'^{(-)}\sigma' \mid v \mid \vec{k}''\sigma'' \rangle \ ,$$

and $f_{k''\sigma''}$ is the Fermi occupation factor for the intermediate states $\mid k''\sigma'' \rangle$.

The term in Eq. (2.17) containing the commutator gives only a spin-dependent contribution to the resistivity. This term does not enter our calculations; as we will see the spin-dependent part of the resistivity ρ_b has to be evaluated to first order only since it enters squared in the expression for the total resistivity.

By rewriting the first term in Eq. (2.17) in terms of $\mid jm_j \rangle$ states we find

$$dT^{(2)}_{\vec{k}\sigma,\vec{k}'\sigma'} = \frac{4}{\Delta N(E_F)} \sum_{jj'} \sum_{\substack{m_3 \\ m_4}}{}' \exp[i(\eta_j + \eta_{j'})] \sin\eta_j \sin\eta_{j'} \langle m_4\sigma' \mid j'm_{j'} \rangle \langle j'm_{j'} \mid vGv \mid jm_j \rangle \times \langle jm_j \mid m_3\sigma \rangle Y_{m_4}(\Omega_{\vec{k}'}) Y_{m_3}(\Omega_{\vec{k}}) \ , \tag{2.18}$$

where

$$m_j = m_3 + \sigma \ ,$$

$$m_{j'} = m_4 + \sigma' \ ,$$

and

$$\langle j'm_{j'} \mid vGv \mid jm_j \rangle = -\sum_{j''m''} \frac{e^{i\eta_{j''}}}{\Delta} \sin\eta_{j''} \langle j'm_{j'} \mid v \mid j''m_{j''} \rangle \langle j''m_{j''} \mid v \mid jm_j \rangle \ . \tag{2.19}$$

III. CALCULATION OF TRANSPORT AND EPR PROPERTIES

A. Transport properties

The magnetoresistance and the extraordinary Hall resistivity for a given spin direction (σ) can be written as[8]

$$\rho^{(\sigma)}_{\vec{u}} = \left[\frac{\hbar}{8\pi^3 ne} \right] \times \sum_{\sigma'} \int \frac{f^0_k(1 - f^0_{k'})}{k_B T} (\vec{k}\cdot\vec{u}) \times [(\vec{k} - \vec{k}')\cdot\vec{u}] W^s_{\vec{k}\sigma\to\vec{k}'\sigma'} d^3k \, d^3k' \tag{3.1}$$

and

$$\rho^{(\sigma)}_{xy} = -\left[\frac{\hbar}{8\pi^3 ne} \right] \int \left[-\frac{\partial f^0_k}{\partial \epsilon_k} \right] (\vec{k}\cdot\vec{u})(\vec{k}'\cdot\vec{v}) \times W^A_{\vec{k}\sigma\to\vec{k}'\sigma} d^3k \, d^3k' \ , \tag{3.2}$$

where $W^S_{\vec{k}\sigma\to\vec{k}'\sigma'}$ and $W^A_{\vec{k}\sigma\to\vec{k}'\sigma'}$ are the symmetric and antisymmetric parts of the transition probability Eq. (2.8); $\vec{u}$ and $\vec{v}$ are unit vectors, $\vec{u}$ in the direction of the current and $\vec{v}$ perpendicular to it, and n is the number of conduction electrons per unit volume for one spin direction. Equation (3.2) is for elastic scattering only; the more complex expression for inelastic scattering is not needed.

We write the resistivity $\rho_{\vec{u}}^{(\sigma)}$ which depends on the direction of the spin σ and the current $\vec{u}$ as follows:

$$\rho_{\vec{u}}^{(\pm)}=\rho_a \pm \rho_b \ . \tag{3.3}$$

In a polycrystal (isotropic medium) the dependence of the resistivity, i.e., $\rho_{\vec{u}}^{(\pm)}, \rho_a, \rho_b$, on $\vec{u}$ can be simply expressed as a function of the angle θ between $\vec{u}$ and the magnetic field $\vec{H}$. All resistivities can be written as

$$\rho=\rho_{(H)}^{\text{iso}}+\rho_{(H)}^{\text{aniso}} \ , \tag{3.4}$$

where $\rho_{(H)}^{\text{iso}}$ is independent of θ (depends only on the magnitude of the field) while $\rho_{(H)}^{\text{aniso}}$ is proportional to $(\cos^2\theta-\frac{1}{3})$.

By using Eqs. (2.8), (2.15), (2.16), and (2.18) with Eqs. (3.1) and (3.2), we can calculate ρ_a^{iso}, ρ_a^{aniso}, ρ_b^{iso}, ρ_b^{aniso}, and $\rho_{xy}^{(\pm)}$. For each of these terms we will write successively the contributions coming from the various terms in the scattering probability Eq. (2.8), i.e., from $|T^{(0)}|^2$, $T^{(0)*}dT^{(1)}+\text{c.c.}$, $|dT^{(1)}|^2$, and $T^{(0)*}dT^{(2)}+\text{c.c.}$ We will give only the terms different from zero.

1. $\rho(|T^{(0)}|^2)$

Isotropic term, spin-independent part

$$\begin{aligned}\rho_a(|T^{(0)}|^2)=D[&\sin^2(\eta_0-\eta_1)+\tfrac{4}{5}\sin^2\eta_1\\&+\tfrac{4}{5}\sin^2(\eta_{3/2}-\eta_1)\\&+\tfrac{2}{5}\sin^2(\eta_{1/2}-\eta_1)\\&+\tfrac{6}{5}\sin^2\eta_{3/2}+\tfrac{3}{5}\sin^2\eta_{1/2}] \ ,\end{aligned} \tag{3.5}$$

where

$$D=\frac{2mc}{\pi\hbar n e^2 n(E_F)} \ , \tag{3.6}$$

c is the concentration of rare-earth impurities and $n(E_F)$ is the density of states at the Fermi level per atom and for one spin direction.

2. $\rho(T^{(0)*}dT^{(1)}+c.c.)$

a. Anisotropic term, spin-independent part

$$\begin{aligned}\rho_a^{\text{aniso}}(T^{(0)*}dT^{(1)}+\text{c.c.})=\frac{8D}{7}\frac{\langle 0_0^2\rangle}{\Delta}\{&[\cos\eta_{1/2}\sin^2\eta_{3/2}\sin\eta_{1/2}+\cos\eta_{3/2}\sin\eta_{3/2}\sin^2\eta_{1/2}\\&+\tfrac{7}{15}\sin\eta_{3/2}\sin\eta_{1/2}\sin\eta_1\cos(\eta_{1/2}+\eta_{3/2}-\eta_1)]\tilde{A}_5\\&+[\cos\eta_{3/2}\sin^3\eta_{3/2}+\tfrac{7}{30}\sin\eta_1\sin^2\eta_{3/2}\cos(2\eta_{3/2}-\eta_1)]\tilde{A}_6\} \ ,\end{aligned} \tag{3.7}$$

where

$$0_0^2=(3/2)^{1/2}[J_{\vec{u}}^2-\tfrac{1}{3}J(J+1)] \ ,$$

$$\tilde{A}_5=\tfrac{3}{2}\mathscr{P}_3A_3+\tfrac{1}{2}\mathscr{P}_4A_4+\tfrac{1}{2}\mathscr{P}_5A_5 \ ,$$

and

$$\tilde{A}_6=\tfrac{3}{2}\mathscr{P}_3A_3-\mathscr{P}_4A_4-\mathscr{P}_5A_5 \ .$$

b. Anisotropic term, spin-dependent part

$$\begin{aligned}\rho_b^{\text{aniso}}(T^{(0)*}dT^{(1)}+\text{c.c.})=\frac{8D\langle J_Z\rangle}{21\Delta}\Big[&(\tilde{A}_3-\tfrac{3}{2}\tilde{A}_4)\sin^3\eta_{3/2}\cos\eta_{3/2}-\tilde{A}_1\sin^3\eta_{1/2}\cos\eta_{1/2}\\&+\frac{1}{2\sqrt{2}}\tilde{A}_2(\sin^2\eta_{1/2}\sin2\eta_{3/2}+\sin^2\eta_{3/2}\sin2\eta_{1/2})\Big] \ ,\end{aligned} \tag{3.8}$$

where

$$\tilde{A}_1=-\tfrac{1}{3}\mathscr{P}_0A_0-\tfrac{4}{3}\mathscr{P}_1A_1-2\mathscr{P}_2A_2 \ ,$$

$$\tilde{A}_2=-\sqrt{2}(\tfrac{1}{3}\mathscr{P}_0A_0+\tfrac{1}{3}\mathscr{P}_1A_1-\tfrac{1}{4}\mathscr{P}_2A_2)\ ,$$
$$\tilde{A}_3=\tfrac{1}{3}\mathscr{P}_0A_0-\tfrac{2}{3}\mathscr{P}_1A_1+\tfrac{1}{5}\mathscr{P}_2A_2\ ,$$

and

$$\tilde{A}_4=\frac{54}{5}\mathscr{P}_2A_2\ .$$

c. Isotropic term, spin-dependent part

$$\begin{aligned}\rho_b^{\rm iso}(T^{(0)*}dT^{(1)}+\text{c.c.})=\frac{D\langle J_Z\rangle}{3\Delta}\Big[&10\tilde{A}_3\sin^3\eta_{3/2}\cos\eta_{3/2}-\tilde{A}_1\sin^3\eta_{1/2}\cos\eta_{1/2}\\&-2\sqrt{2}\tilde{A}_2(\sin^2\eta_{1/2}\sin2\eta_{3/2}+\sin^2\eta_{3/2}\sin2\eta_{1/2})\\&+\tfrac{2}{5}\sin\eta_1[-10\tilde{A}_3\cos(2\eta_{3/2}-\eta_1)\sin^2\eta_{3/2}\\&+\frac{8}{\sqrt{2}}\tilde{A}_2\sin\eta_{1/2}\sin\eta_{3/2}\cos(\eta_{3/2}+\eta_{1/2}-\eta_1)\\&+\tilde{A}_1\sin^2\eta_{1/2}\cos(2\eta_{1/2}-\eta_1)]\Big]\end{aligned}\tag{3.9}$$

3. $\rho(|dT^{(1)}|^2)$

a. Anisotropic term, spin-independent part

$$\begin{aligned}\rho_a^{\rm aniso}(|dT^{(1)}|^2)=\frac{3D}{7\Delta^2}&(\langle J_{\vec{u}}WJ_{\vec{u}}\rangle-\tfrac{1}{3}\langle\vec{\mathrm{J}}\cdot W\vec{\mathrm{J}}\rangle)\\&\times[(2\tilde{A}_3^2-\tilde{A}_4\tilde{A}_3-\tfrac{2}{9}\tilde{A}_4^2)\sin^4\eta_{3/2}-\tilde{A}_2^2\sin^2\eta_{1/2}\sin^2\eta_{3/2}\\&+\sqrt{2}\tilde{A}_1\tilde{A}_2\sin^3\eta_{1/2}\sin\eta_{3/2}\cos(\eta_{3/2}-\eta_{1/2})\\&+\sqrt{2}\tilde{A}_2(\tilde{A}_3+\tilde{A}_4)\sin\eta_{1/2}\sin^3\eta_{3/2}\cos(\eta_{3/2}-\eta_{1/2})]\ ,\end{aligned}\tag{3.10}$$

where

$$\langle\vec{\mathrm{J}}\cdot W\vec{\mathrm{J}}\rangle=\sum_{\alpha\beta}P_{(\alpha)}\frac{(E_\alpha-E_\beta)/k_BT}{1-\exp\left[-\left[\dfrac{(E_\alpha-E_\beta)}{k_BT}\right]\right]}\langle\alpha|\vec{\mathrm{J}}|\beta\rangle\cdot\langle\beta|\vec{\mathrm{J}}|\alpha\rangle\tag{3.11}$$

and

$$P_{(\alpha)}=\frac{1}{Z}\exp(-E_\alpha/k_BT)\ .$$

b. Isotropic term, spin-independent part

$$\begin{aligned}\rho_a^{\rm iso}(|dT^{(1)}|^2)=&\frac{D\langle\vec{\mathrm{J}}\cdot W\vec{\mathrm{J}}\rangle}{4\Delta^2}[(10\tilde{A}_3^2+\tfrac{10}{9}\tilde{A}_4^2)\sin^4\eta_{3/2}+\tilde{A}_1^2\sin^4\eta_{1/2}+8\tilde{A}_2^2\sin^2\eta_{1/2}\sin^2\eta_{3/2}]\\&+\frac{D}{\Delta^2}\langle O^2\cdot WO^2\rangle(2\tilde{A}_6^2\sin^4\eta_{3/2}+4\tilde{A}_5^2\sin^2\eta_{3/2}\sin^2\eta_{1/2})\ .\end{aligned}\tag{3.12}$$

4. $\rho(T^{(0)*}dT^{(2)}+c.c.)$

Anisotropic term, spin-independent part

$$\rho_a^{\text{aniso}}(T^{(0)*}dT^{(2)}+\text{c.c.})$$
$$=\frac{6D}{7\Delta^2}\langle J_{\vec{u}}^2-\tfrac{1}{3}J(J+1)\rangle$$
$$\times\left[\frac{1}{\sqrt{2}}\tilde{A}_1\tilde{A}_2\cos2\eta_{1/2}\sin^2\eta_{1/2}\sin^2\eta_{3/2}+\frac{1}{\sqrt{2}}\tilde{A}_2(\tilde{A}_3+\tilde{A}_4)\cos(\eta_{1/2}+\eta_{3/2})\sin^3\eta_{3/2}\sin\eta_{1/2}\right.$$
$$+\frac{1}{\sqrt{2}}\tilde{A}_1\tilde{A}_2\cos(\eta_{1/2}+\eta_{3/2})\sin^3\eta_{1/2}\sin\eta_{3/2}+\frac{1}{\sqrt{2}}\tilde{A}_2(\tilde{A}_3+\tilde{A}_4)\cos2\eta_{3/2}\sin^2\eta_{3/2}\sin^2\eta_{1/2}$$
$$\left.+(2\tilde{A}_3^2-\tilde{A}_4\tilde{A}_3-\tfrac{2}{9}\tilde{A}_4^2)\sin^4\eta_{3/2}\cos2\eta_{3/2}-\tilde{A}_2^2\cos(\eta_{1/2}+\eta_{3/2})\sin\eta_{1/2}\sin^3\eta_{3/2}\right]. \tag{3.13}$$

5. $\rho_{xy}(T^{(0)*}dT^{(1)}+c.c.)$

$$\rho_{xy}^{\pm}=-\frac{D\sin\eta_1}{\Delta}\langle J_Z\rangle\left[\frac{A_0(g_J-1)}{3}[\sin^2\eta_{3/2}\sin(2\eta_{3/2}-\eta_1)-\tfrac{1}{5}\sin^2\eta_{1/2}\sin(2\eta_{1/2}-\eta_1)\right.$$
$$-\tfrac{4}{5}\sin\eta_{1/2}\sin\eta_{3/2}\sin(\eta_{1/2}+\eta_{3/2}-\eta_1)]$$
$$-\tfrac{2}{3}A_1(2-g_J)[\sin^2\eta_{3/2}\sin(2\eta_{3/2}-\eta_1)+\tfrac{2}{5}\sin^2\eta_{1/2}\sin(2\eta_{1/2}-\eta_1)$$
$$\left.+\tfrac{2}{5}\sin\eta_{1/2}\sin\eta_{3/2}\sin(\eta_{1/2}+\eta_{3/2}-\eta_1)]\right]. \tag{3.14}$$

The total resistivity is then calculated as follows in a two-current model.[8] With our assumption of scattering due to v restricted to the $l=2$ channel, there is no momentum transfer between the spin-up and spin-down currents, i.e., $\rho_{\uparrow\downarrow}=0$ in the notation of Ref. 8, so that the total resistivity can be written as

$$\rho_{\vec{u}}=\frac{\rho_{\vec{u}}^{(+)}\rho_{\vec{u}}^{(-)}}{\rho_{\vec{u}}^{(+)}+\rho_{\vec{u}}^{(-)}}. \tag{3.15}$$

By using Eq. (3.3), we find

$$\rho_{\vec{u}}=\frac{\rho_a}{2}-\frac{\rho_b^2}{2\rho_a}. \tag{3.16}$$

For zero magnetic field ρ_b is zero, so that the zero-field resistivity is written as

$$\rho_0=\frac{\rho_a(H=0)}{2}. \tag{3.17}$$

By keeping only the dominant contribution to ρ_a, i.e., that coming from $|T^{(0)}|^2$, Eq. (3.5), we find

$$\rho_0=\tfrac{1}{2}\rho(|T^{(0)}|^2). \tag{3.18}$$

The isotropic and anisotropic magnetoresistances are found by writing ρ_a and ρ_b in Eq. (3.16) as the sum of their isotropic and anisotropic parts. We obtain

$$\frac{\Delta\rho^{\text{iso}}}{\rho_0}\equiv\frac{\rho_{\vec{u}}^{\text{iso}}-\rho_0}{\rho_0}$$
$$=\frac{\rho_a^{\text{iso}}(H)-\rho_a^{\text{iso}}(H=0)}{\rho_a(|T^0|^2)}$$
$$-\left[\frac{\rho_b^{\text{iso}}}{\rho_a(|T^{(0)}|^2)}\right]^2, \tag{3.19}$$

and

$$\frac{\rho_{\vec{u}}^{\text{aniso}}}{\rho_0}=\frac{\rho_a^{\text{aniso}}}{\rho_a(|T^{(0)}|^2)}-\frac{2\rho_b^{\text{aniso}}}{\rho_b^{\text{iso}}}\left[\frac{\rho_b^{\text{iso}}}{\rho_a(|T^{(0)}|^2)}\right]^2-\left[\frac{\rho_b^{\text{aniso}}}{\rho_b^{\text{iso}}}\right]^2\left[\frac{\rho_b^{\text{iso}}}{\rho_a(|T^{0}|^2)}\right]^2 . \tag{3.20}$$

The dependence of $\Delta\rho^{\text{iso}}$ on H for non-S-state impurities is rather complicated since it contains terms proportional to

$$(\langle\vec{J}\cdot W\vec{J}\rangle-\langle\vec{J}\cdot W\vec{J}\rangle_{H=0})$$

and

$$(\langle O^2\cdot WO^2\rangle-\langle O^2\cdot WO^2\rangle_{H=0})$$

arising from ρ_a^{iso}, as well as terms proportional to $(\langle J_Z\rangle)^2$ coming from ρ_b^2. The expectation values of $\langle\vec{J}\cdot W\vec{J}\rangle$, $\langle O^2\cdot WO^2\rangle$, and $\langle J_Z\rangle$ have been computed by Ousset *et al.*[9] for several alloys with the appropriate crystal-field parameters. They found that, for non-S-state ions, $\Delta\rho^{\text{iso}}$ is the sum of positive and negative terms, nearly canceling each other for certain crystal-field schemes, which makes it difficult to interpret the experimental data.

On the other hand, for Gd impurities (S-state ion) the expression of $\Delta\rho^{\text{iso}}$ can be greatly simplified. In the absence of crystal-field splitting, one obtains by a straightforward calculation[10]

$$\langle\vec{J}\cdot W\vec{J}\rangle=J(J+1)-|\langle J_Z\rangle|\left[\coth\frac{\alpha}{2}-\frac{\alpha/2}{\sinh^2\frac{\alpha}{2}}\right], \tag{3.21}$$

where

$$\alpha=\frac{g_J\mu_B H}{k_B T} .$$

In this case $\Delta\rho^{\text{iso}}$ can be written as

$$\Delta\rho^{\text{iso}}=-\gamma\langle J_Z\rangle^2-\beta|\langle J_Z\rangle|\left[\coth\alpha/2-\frac{\alpha/2}{\sinh^2\frac{\alpha}{2}}\right], \tag{3.22}$$

where

$$\gamma=\frac{D^2A_0^2(g_J-1)^2}{162\Delta^2\rho_a(|T_0|^2)}\{10\sin^3\eta_{3/2}\cos\eta_{3/2}+\sin^3\eta_{1/2}\cos\eta_{1/2}+4\sin^2\eta_{1/2}\sin2\eta_{3/2}+4\sin^2\eta_{3/2}\sin2\eta_{1/2}$$
$$-\tfrac{2}{5}\sin\eta_1[10\cos(2\eta_{3/2}-\eta_1)\sin^2\eta_{3/2}+8\sin\eta_{1/2}\sin\eta_{3/2}\cos(\eta_{3/2}+\eta_{1/2}-\eta_1)$$
$$-\sin^2\eta_{1/2}\cos(2\eta_{1/2}-\eta_1)]\}^2 , \tag{3.23}$$

and

$$\beta=\frac{DA_0^2(g_J-1)^2}{72\Delta^2}(10\sin^4\eta_{3/2}+\sin^4\eta_{1/2}+16\sin^2\eta_{1/2}\sin^2\eta_{3/2}) . \tag{3.24}$$

The anisotropic part of $\rho_{\vec{u}}$ also includes several terms that we have computed. It appears that, in the range of phase shifts consistent with the experimental data, the contribution from $\rho_a^{\text{aniso}}(T^{(0)*}dT^{(1)}+\text{c.c.})$ is larger than the others by at least 2 orders of magnitude. Thus we can limit the expression of $\rho_{\vec{u}}^{\text{aniso}}$ to this term. Rather than $\rho_{\vec{u}}^{\text{aniso}}$ we will write the expression of the anisotropy of the resistivity as

$$\frac{\rho_{||}-\rho_\perp}{\rho_0} ,$$

which is the quantity conventionally used to present the experimental data on anisotropy.[11] For a polycrystalline sample we have from Eq. (3.16),

$$\frac{\rho_{||}-\rho_\perp}{\rho_0}=\frac{3}{2}\frac{\rho_{(\vec{H}||\vec{u})}^{\text{aniso}}}{\rho_0}=\frac{3}{4}\frac{\rho_{a(\vec{H}||\vec{u})}^{\text{aniso}}}{\rho_0} . \tag{3.25}$$

From Eq. (3.7) we obtain

$$\frac{\rho_{||}-\rho_\perp}{\rho_0}=a\left[\langle\langle J_Z^2\rangle\rangle-\frac{J(J+1)}{3}\right], \tag{3.26}$$

where

$$a=\frac{3}{7}\frac{\sqrt{6}D}{\Delta\rho_0}\{[\cos\eta_{1/2}\sin^2\eta_{3/2}\sin\eta_{1/2}+\cos\eta_{3/2}\sin\eta_{3/2}\sin^2\eta_{1/2}$$
$$+\tfrac{7}{15}\sin\eta_{3/2}\sin\eta_{1/2}\sin\eta_1\cos(\eta_{1/2}+\eta_{3/2}-\eta_1)]\tilde{A}_5$$
$$+[\cos\eta_{3/2}\sin^3\eta_{3/2}+\tfrac{7}{30}\sin\eta_1\sin^2\eta_{3/2}\cos(2\eta_{3/2}-\eta_1)]\tilde{A}_6\}\ , \tag{3.27}$$

J_Z is the component of $\vec{J}$ along the field direction, and $\langle\langle J_Z^2\rangle\rangle$ is a thermal and powder average of J_Z^2.

In the two-current model, the extraordinary Hall resistivity is written as[3]

$$\rho_{xy}^E=\tfrac{1}{4}(\rho_{xy}^+ +\rho_{xy}^-)\ , \tag{3.28}$$

where $\rho_{xy}^{(\pm)}$ are given by Eq. (3.14). At sufficiently high temperature we can write

$$\langle J_Z\rangle=-\frac{g_J J(J+1)\mu_B H}{3k_B T}\ ,$$

so that ρ_{xy}^E/ρ_0 can be written as

$$\frac{\rho_{xy}^E}{\rho_0}=[\alpha_1 g_J(2-g_J)J(J+1)+\alpha_2 g_J(g_J-1)J(J+1)]\frac{H}{T}\ , \tag{3.29}$$

where

$$\alpha_1=\frac{\mu_B A_1 D}{9\Delta k_B\rho_0}\sin\eta_1[\sin^2\eta_{3/2}(2\eta_{3/2}-\eta_1)+\tfrac{2}{5}\sin^2\eta_{1/2}\sin(2\eta_{1/2}-\eta_1)$$
$$+\tfrac{2}{5}\sin\eta_{1/2}\sin\eta_{3/2}\sin(\eta_{1/2}+\eta_{3/2}-\eta_1)]\ , \tag{3.30}$$

and

$$\alpha_2=-\frac{\mu_B D A_0\sin\eta_1}{18\Delta k_B\rho_0}[\sin^2\eta_{3/2}\sin(2\eta_{3/2}-\eta_1)-\tfrac{1}{5}\sin^2\eta_{1/2}\sin(2\eta_{1/2}-\eta_1)$$
$$-\tfrac{4}{5}\sin\eta_{1/2}\sin\eta_{3/2}\sin(\eta_{1/2}+\eta_{3/2}-\eta_1)]\ . \tag{3.31}$$

The first term α_1 is proportional to the oribtal exchange coefficient A_1 and exists only for non-S-state ions ($g\neq 2$). The second term α_2 is proportional to the spin exchange coefficient A_0 and results from the spin-orbit splitting of the VBS. It exists even for Gd but cancels when $\eta_{3/2}=\eta_{1/2}$, i.e., no spin-orbit splitting of VBS.

B. Evaluation of the g shift and EPR linewidth

We will now derive expressions for the g shift Δg and linewidth ΔH in terms of the same parameters used in the resistivity calculation. The transition probability between two states of the $4f$ conduction-electron system is given by

$$W_{\alpha\vec{k}\sigma\to\beta\vec{k}'\sigma'}=\frac{2\pi}{\hbar}\,|\,T_{\alpha\vec{k}\sigma\to\beta\vec{k}'\sigma'}\,|^2\delta_{(\epsilon_{k\sigma}-\epsilon_{k'\sigma'}+E_\alpha-E_\beta)}\ , \tag{3.32}$$

where α,β are the $4f$ states and $\vec{k}\sigma,\vec{k}'\sigma'$ the $5d$ (VBS) states. Summing over all the possible states of the conduction electron we find

$$W_{\alpha\to\beta}=\frac{2\pi}{\hbar}\sum_{\sigma\sigma'}\int k^2dk\int k'^2dk' f_{(k\sigma)}(1-f_{(k'\sigma')})\int d\Omega_k\int d\Omega_{k'}\,|\,T_{\alpha\vec{k}\sigma\to\beta\vec{k}'\sigma'}\,|^2\delta_{(\epsilon_{k\sigma}-\epsilon_{k'\sigma'}+E_\alpha-E_\beta)}\ . \tag{3.33}$$

By replacing the integral over k by one over energy ϵ_k

$$\int k^2 dk \to \int \frac{N(\epsilon_k) d\epsilon_k}{4\pi} ,$$

and taking into account that for $\mu_B H \ll k_B T$ we can neglect $E_\alpha - E_\beta$ in the argument of f and N, we can write the transition probability Eq. (3.33) as

$$W_{\alpha\to\beta} = \frac{k_B T}{8\pi\hbar} N^2(E_F) \times \sum_{\sigma\sigma'} \int_{\Omega_k} \int_{\Omega_{k'}} | T_{\alpha \vec{k}\sigma \to \beta \vec{k}'\sigma'} |^2 d\Omega_k d\Omega_{k'} . \tag{3.34}$$

If we note that

$$\sum_{\sigma'} \int_{\Omega_{\vec{k}}} \int_{\Omega_{\vec{k}'}} | T_{\alpha \vec{k}\sigma \to \beta \vec{k}'\sigma'} |^2 d\Omega_k d\Omega_{k'} \equiv R_a^{\rm iso} \tag{3.35}$$

is the same angular integration that gives us the isotropic magnetoresistance, we obtain

$$W_{\alpha\to\beta} = \frac{k_B T}{4\pi\hbar} N^2(E_F) R_a^{\rm iso} , \tag{3.36}$$

where, from Eq. (3.12)

$$R_a^{\rm iso} = \frac{4}{\Delta^2 N^2(E_F)} \langle \alpha | \vec{J} | \beta \rangle \langle \beta | \vec{J} | \alpha \rangle \times (10 \tilde{A}_3^2 \sin^4 \eta_{3/2} + \tilde{A}_1^2 \sin^4 \eta_{1/2} + 8 \tilde{A}_2^2 \sin^2 \eta_{1/2} \sin^2 \eta_{3/2}) . \tag{3.37}$$

The relaxation time T_1 is given by[12]

$$\frac{1}{T_1} = \frac{1}{2} \frac{\sum_{\alpha,\beta} W_{\alpha\to\beta} (E_\alpha - E_\beta)^2}{\sum_\alpha E_\alpha^2} . \tag{3.38}$$

For a doublet this is just

$$\frac{1}{T_1} = W_{\alpha\to\beta} + W_{\beta\to\alpha} ,$$

and since we consider $W_{\alpha\to\beta} \simeq W_{\beta\to\alpha}$ we have

$$\frac{1}{T_1} = 2 W_{\alpha\to\beta} , \tag{3.39}$$

and the resonance width is

$$\frac{\Delta H}{\Delta T} = \frac{\hbar}{g\mu_B} \frac{1}{T_1 T} = \frac{2\hbar W_{\alpha\to\beta}}{g\mu_B T} . \tag{3.40}$$

For an isotropic doublet,

$$\langle \alpha | \vec{J} | \beta \rangle \langle \beta | \vec{J} | \alpha \rangle = \frac{1}{2} \left[\frac{g}{g_J} \right]^2 ,$$

and we find from Eqs. (3.36) and (3.40)

$$\frac{\Delta H}{\Delta T} = \frac{k_B g}{\pi \mu_B \Delta^2 g_J^2} (10 \tilde{A}_3^2 \sin^4 \eta_{3/2} + \tilde{A}_1^2 \sin^4 \eta_{1/2} + 8 \tilde{A}_2^2 \sin^2 \eta_{3/2} \sin^2 \eta_{1/2}) . \tag{3.41}$$

For Gd, if we take as the ground state a pure $J = \frac{7}{2}$ state, we have eight levels $| \frac{7}{2} m_j \rangle$. The dominant part of the interaction v Eq. (2.14), i.e., the bilinear spin exchange, only connects adjacent levels and we can write

$$\frac{1}{T_1} = \frac{1}{2} \frac{\sum_{n,n'} W_{n\to n'} (E_n - E_{n'})^2}{\sum_n E_n^2} = \frac{\sum_n W_{n\to n+1}}{42} , \quad n' = n \pm 1 . \tag{3.42}$$

By using Eqs. (3.36), (3.37), (3.40), and

$$\langle \tfrac{7}{2} m_j | \vec{J} | \tfrac{7}{2} m_j + 1 \rangle \langle \tfrac{7}{2} m_j + 1 | \vec{J} | \tfrac{7}{2} m_j \rangle = \tfrac{1}{2} (\tfrac{9}{2} + m_j) (\tfrac{7}{2} - m_j) ,$$

we obtain for Gd the following:

$$\frac{\Delta H}{\Delta T} = \frac{k_B A_0^2}{18\pi\mu_B \Delta^2} (10 \sin^4 \eta_{3/2} + \sin^4 \eta_{1/2} + 16 \sin^2 \eta_{3/2} \sin^2 \eta_{1/2}) . \tag{3.43}$$

To obtain the g shift produced by the local-moment–conduction-electron interaction we have to evaluate the thermal average of the conduction-electron operators appearing in the interaction in the presence of a magnetic field. The average values of the conduction-electron operators are given in linear-response theory as[12]

$$\langle \vec{l} \rangle = \sum_{\alpha,\beta} \langle \alpha | \vec{l} | \beta \rangle \langle \beta | -\mu_B \vec{H} \cdot \vec{l} - 2\mu_B \vec{H} \cdot \vec{s} | \alpha \rangle \times S(\alpha,\beta,0) , \tag{3.44}$$

$$\langle \vec{s} \rangle = \sum_{\alpha,\beta} \langle \alpha | \vec{s} | \beta \rangle \langle \beta | -\mu_B \vec{H} \cdot \vec{I} - 2\mu_B \vec{H} \cdot \vec{s} | \alpha \rangle \times S(\alpha,\beta,0) , \quad (3.45)$$

where α,β are the states of the system. The static susceptibility $S(\alpha,\beta,0)$ is given by[13]

$$S(\tfrac{3}{2},\tfrac{3}{2},0) = \frac{\sin^2\eta_{3/2}}{\pi\Delta} ,$$
$$S(\tfrac{1}{2},\tfrac{1}{2},0) = \frac{\sin^2\eta_{1/2}}{\pi\Delta} , \quad (3.46)$$
$$S(\tfrac{3}{2},\tfrac{1}{2},0) = \frac{\sin\eta_{3/2}\sin\eta_{1/2}}{\pi\Delta} .$$

If we restrict the exchange interaction to the first two terms in Eq. (2.14) the g shift is given by[13]

$$\Delta g = \frac{1}{\mu_B H_Z} \left[-\frac{A_0(g_J-1)}{g_J} \langle s_Z \rangle - \frac{A_1(2-g_J)g}{g_J} \langle l_Z \rangle \right] , \quad (3.47)$$

and by using Eqs. (3.44), (3.45), and (3.46) we find

$$\Delta g = \frac{A_0(g_J-1)g}{\pi g_J \Delta} \left(\tfrac{5}{3}\sin^2\eta_{3/2} - \tfrac{2}{9}\sin^2\eta_{1/2} + \tfrac{14}{9}\sin\eta_{3/2}\sin\eta_{1/2} \right) + \frac{A_1(2-g_J)g}{\pi g_J \Delta} \left(\tfrac{10}{3}\sin^2\eta_{3/2} + \tfrac{2}{9}\sin^2\eta_{1/2} + \tfrac{4}{9}\sin\eta_{1/2}\sin\eta_{3/2} \right) . \quad (3.48)$$

IV. COMPARISON WITH EXPERIMENTAL RESULTS

A. Transport properties

In order to test the model in the most detailed way, we have gathered data from several types of measurements: residual resistivity,[14,15] thermoelectric power,[16,17] isotropic and anisotropic magnetoresistances,[11] and Hall effect.[3] We distinguish two sort of properties: (i) those which depend essentially on the VBS parameters, i.e., phase shifts, and (ii) those which also depend on the parameters associated with the $4f$-$5d$ interaction, i.e., the parameters A_0, A_1, etc., which are combinations of $4f$-$5d$ Slater-type integrals.

We begin by considering experimental data on the properties of the first of these categories in order to obtain reliable estimates of the phase shifts in the model: η_0, η_1, $\eta_{1/2}$, and $\eta_{3/2}$. We could determine these phase shifts for each alloy, that is, one set for Au:Gd, another for Au:Tb, etc. However, we find a reasonably good agreement with the experimental data for *all* the heavy rare-earth metals ($\mathscr{R}$) in a given host can be obtained with a unique set of phase shifts. Thus, for simplicity, we shall assume that the phase shifts are the same for all the heavy $\mathscr{R}$ elements in a given host.

The first condition imposed on the phase shifts arises from the Friedel sum rule[6] which, for a trivalent ion in a monovalent noble metal ($\Delta Z = 2$), is written as

$$\eta_0 + 3\eta_1 + \eta_{1/2} + 2\eta_{3/2} = \pi . \quad (4.1)$$

The residual resistivity of the alloys is the first piece of experimental data we use. The theoretical expression of the residual resistivity is written as [see Eqs. (3.5) and (3.18)]:

$$\rho_0 = \frac{mc}{\pi n e^2 \hbar n(E_F)} \left[\sin^2(\eta_0-\eta_1) + \tfrac{4}{5}\sin^2\eta_1 + \tfrac{2}{5}\sin^2(\eta_{1/2}-\eta_1) + \tfrac{6}{5}\sin^2\eta_{3/2} + \tfrac{3}{5}\sin^2\eta_{1/2} \right] . \quad (4.2)$$

The experimental values for heavy rare-earth impurities are $5.2\ \mu\Omega\,\text{cm/at.}\% < \rho_0 < 6.6\ \mu\Omega\,\text{cm/at.}\%$ for Ag:$\mathscr{R}$ (Ref. 14), and $\rho_0 \simeq 7\ \mu\Omega\,\text{cm/at.}\%$ for Au:$\mathscr{R}$ (Ref. 15).

The second set of experimental data to determine the phase shifts comes from data on the thermoelectric power (TEP) of Ag:Lu and Au:Lu alloys, $A \equiv S/T = 1.79\times10^{-8}\ \text{V K}^{-2}$ for Ag:Lu,[16] and $A = 1.1\times10^{-8}\ \text{V K}^{-2}$ for Au:Lu.[17] For alloys with Lu there is no anomalous contribution to the TEP from inelastic k-f scattering and the TEP at low temperature can be ascribed to the formation of a VBS.[17] The general expression for A is given as

$$A=\frac{\pi^2 k_B^2 T}{3|e|}\left[\frac{\partial \ln \rho_0}{\partial \epsilon}\right]_{E_F}, \tag{4.3}$$

where ρ_0 is given by Eq. (4.2). The only phase shifts which strongly depend on the electron energy ϵ are those associated with the narrow d VBS (i.e., $\eta_{1/2}$ and $\eta_{3/2}$), so that we can neglect the contributions from the $l=0$ and $l=1$ channels. By using Eqs. (4.2) and (4.3) and from the definition of the phase shift η_j,

$$\frac{\partial \eta_j}{\partial \epsilon}=\frac{\sin^2 \eta_j}{\Delta},$$

we obtain

$$\begin{aligned} A=\frac{\pi^2 k_B^2 D}{6|e|\Delta\rho_0}\Big[&\tfrac{4}{5}\sin 2(\eta_{3/2}-\eta_1)\sin^2\eta_{3/2} \\ &+\tfrac{2}{5}\sin 2(\eta_{1/2}-\eta_1)\sin^2\eta_{1/2} \\ &+\tfrac{6}{5}\sin 2\eta_{3/2}\sin^2\eta_{3/2} \\ &+\tfrac{3}{5}\sin 2\eta_{1/2}\sin^2\eta_{1/2}\Big]. \end{aligned} \tag{4.4}$$

The VBS half-width Δ for $5d$ elements in Ag has been determined by optical measurements and by combining thermoelectric power and de Haas–van Alphen data. A reasonable mean value appears to be $\Delta=0.45$ eV. On the other hand, there are no measurements of Δ for $5d$ elements in Au. Information on Δ for the gold-based alloys can be found by comparing the residual resistivities and the TEP of the silver- and gold-based alloys. Their residual resistivities are nearly equal while the TEP of Au:Lu is definitely smaller than that of Ag:Lu (by almost a factor of 2). The only way we can obtain this result is to assume similar phase shifts for the silver- and gold-based alloys with a larger Δ in gold. We have taken $\Delta=0.6$ eV which gives good agreement not only for TEP but also for the whole set of experimental data we consider in this paper. This larger value of Δ may be due to the stronger d character of the conduction electrons in gold. We will discuss this in Sec. V.

In contrast to ρ_0 and A, the magnetoresistance and Hall effect depend on the $4f$-$5d$ interaction coefficients as well as the phase shifts. However, some ratios of experimental quantities give us direct information on the phase shifts alone. We first consider the ratio of the skew scattering coefficients α_1 and α_2. According to Eqs. (3.30) and (3.31), this ratio depends only weakly on η_0, η_1, and $\eta_{3/2}+\eta_{1/2}$ but, as the existence of α_2 results from the spin-orbit splitting of the $5d$ VBS, α_2/α_1 is strongly dependent on the difference $\eta_{3/2}-\eta_{1/2}$. This ratio is also proportional to A_0/A_1 but we can reasonably take for A_0/A_1 the ratio of the atomic values of A_0 and A_1. We show in Fig. 1 an example of the variation of the ratio α_2/α_1 as a function of the spin-orbit splitting parameter,

$$r=\frac{Z_{3/2}}{Z_{1/2}+Z_{3/2}}.$$

The ratio $|\alpha_2/\alpha_1|$ increases from zero for $r=\frac{2}{3}$, which corresponds to an unsplit VBS with $\eta_{3/2}=\eta_{1/2}$, to a value of about 11 for $r=1$ which corresponds to a completely split VBS. This type of graph allows us to derive the splitting parameter r from the experimental values of α_2/α_1; -3.65 for Ag:$\mathscr{R}$ and -6.647 for Au:$\mathscr{R}$. We find that, for both Ag- and Au-based alloys, the splitting is relatively small; $r=0.74$ for Ag:$\mathscr{R}$ and $r=0.83$ for Au:$\mathscr{R}$. As the ratio α_2/α_1 depends weakly on the phase shifts η_0, η_1 and $\eta_{1/2}+\eta_{3/2}$ in the range of values consistent with the Friedel sum rule and the other data, this procedure gives us an almost independent determination of $\eta_{3/2}-\eta_{1/2}$.

Another piece of information on the spin-orbit splitting of the VBS is given by the absence, to within experimental accuracy, of anisotropy of the magnetoresistance in the Gd alloys:

$$\frac{\rho_{\parallel}-\rho_{\perp}}{\Delta\rho^{\mathrm{iso}}}\leq 4\%,$$

in both Ag- and Au-based alloys. According to the results of our calculations of the preceding section, the spin-orbit splitting of the VBS induces an anisotropy of the magnetoresistance for Gd alloys; see Eqs. (3.8), (3.10) and (3.13). In Fig. 1 we also show the value at saturation of the relative anisotropy plotted as a function of the spin-orbit splitting parameter r. The anisotropy is zero for $r=\frac{2}{3}$ (unsplit VBS), it increases very slowly (quadratically in $r-\frac{2}{3}$) and reaches significant values only for strongly split VBS. For the values of r derived from the Hall effect, the anisotropy is negligible, in agreement with the experimental results. Therefore there is no contradiction between the negligible anisotropy of the magnetoresistance and the significant skew scattering of Gd alloys: They are both consistent with a rather small spin-orbit splitting.

Next, we consider, for alloys with Gd impurities, the ratio

$$\alpha_2\Big/\left[\left|\frac{\Delta\rho_{\mathrm{sat}}^{\mathrm{iso}}}{\rho_0}\right|\right]^{1/2},$$

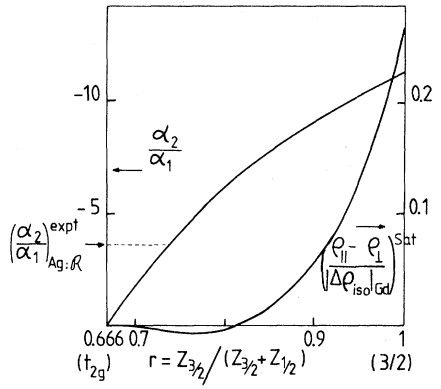

FIG. 1. Variation of the ratio of extraordinary Hall resistivity coefficients α_2/α_1 and of the ratio of anisotropic to isotropic resistivities for Gd as a function of the spin-orbit splitting of the VBS. The curve for $[(\rho_{\parallel}-\rho_{\perp})/(\,|\,\Delta\rho^{iso}\,|\,)]_{Gd}$ differs slightly from that previously shown (see Ref. 18), because differrent values of the phase shifts are used.

where α_2 is the skew scattering coefficient and $\Delta\rho^{iso}_{sat}$ is the value at saturation of the isotropic magnetoresistance. From the expressions for α_2 and $\Delta\rho^{iso}$, Eqs. (3.31) and (3.22), it is seen that this ratio depends only on the phase shifts and not on the $4f$-$5d$ coefficient A_0. Moreover, it can be written as

$$\alpha_2 \Big/ \left[\left|\frac{\Delta\rho^{iso}_{sat}}{\rho_0}\right|\right]^{1/2} = \sin\eta_1 f(\eta_l)\ ,$$

where the function $f(\eta_l)$ does not vary much for the range of phase shifts consistent with other data. Thus, from the experimental value of this ratio,[3,11,18] we obtain an independent and reliable determination of the phase shift η_1.

In Table II we present the two sets of phase shifts adopted for the Ag:$\mathscr{R}$ and Au:$\mathscr{R}$ systems and the corresponding screening charges Z_0, Z_1, $Z_{3/2}$, and $Z_{1/2}$. These phase shifts obey the Friedel sum rule, Eq. (4.1) and give reasonably good agreement for the residual resistivity, the thermoelectric power and the three ratios mentioned above. The calculated and experimental values of these quantities are also listed. All the calculations have been performed with $n(E_F)$ $=0.15$ eV^{-1} per atom for one spin direction.

Having analyzed experimental data on quantities depending only on the phase shifts, we now consider experimental data on properties depending on the $4f$-$5d$ interaction. The anisotropic magnetoresistance induced by non-S-state impurities can be written as (see Sec. III):

$$\frac{\rho_{\parallel}-\rho_{\perp}}{\rho_0} = a\left[\langle\langle J_Z^2\rangle\rangle - \frac{J(J+1)}{3}\right]\ , \tag{4.5}$$

where a is given by Eq. (3.27). Experiments have been analyzed by using Eq. (4.5) and from the fits experimental values of the coefficient a have been derived for most heavy-$\mathscr{R}$ impurities in Ag and Au.[9] When one calculates a by placing in Eq. (4.5) the phase shifts derived above (see Table II) and atomic values of the parameters A_3, A_4, A_5, one obtains value of a somewhat larger than the experimental ones. Good agreement throughout the $\mathscr{R}$ series can be obtained simply by taking effective values of A_3, A_4, A_5 lowered with respect to their atomic values by a factor of about 1.68 for Ag-based alloys and 2.26 for Au-based alloys. The values of the coefficient a calculated with these effective values of A_3, A_4, A_5 are listed in Table IV together with the experimental values of a. The effective and atomic values of A_3, A_4, A_5 are listed in Table V. In Figs. 2 and 3 we plot the variation of the calculated and experimental values of a through the heavy $\mathscr{R}$ series. The variation predicted by our model is slightly different from the variation of the Stevens coefficient α_J, i.e., from that expected from only quadrupole k-f scattering.

TABLE II. Phase shifts giving the best agreement with experimental results; see Table III and corresponding screening charges.

	Ag:$\mathscr{R}$		Au:$\mathscr{R}$	
	η_l	Z_l	η_l	Z_l
$l=0$	1.3	0.83	1.29	0.82
$l=1$	0.181	0.345	0.22	0.42
$\tilde{j}=\frac{1}{2}$	0.34	0.216	0.21	0.13
$\tilde{j}=\frac{3}{2}$	0.478	0.608	0.49	0.62

TABLE III. Calculated and experimental transport properties of Ag:$\mathscr{R}$ and Au:$\mathscr{R}$ alloys. The first five lines have been calculated with the phase shifts of Table II and, for the TEP, with the values of Δ indicated in the text. The skew scattering coefficients α_1 and α_2 have been calculated with the same parameters and the values of A_0 and A_1 given in Table V.

	Ag host		Au host	
	Calculation	Experiment	Calculation	Experiment
(ρ_0) $\mu\Omega$ cm/at.%	5.46	5.2–6	5	7
$(A \equiv S/T)$ V/K^2	1.55×10^{-8}	1.79×10^{-8}	1.137×10^{-8}	1.1×10^{-8}
α_2/α_1	−3.62	−3.65	−6.647	−6.647
$\left[\alpha_2 \Big/ \left[\left\lvert\frac{\Delta\rho^{\rm iso}}{\rho_0}\right\rvert\right]^{1/2}\right]^{\rm sat}_{\rm Gd}$ (K/G)	-1.28×10^{-7}	-1.28×10^{-7}	-3.57×10^{-7}	-3.57×10^{-7}
$\left[\left\lvert\frac{\rho_{\parallel}-\rho_{\perp}}{\Delta\rho^{\rm iso}}\right\rvert\right]^{\rm sat}_{\rm Gd}$	0.007	0.04	0.097	0.04
(α_1) K/G	0.425×10^{-8}	0.43×10^{-8}	0.335×10^{-8}	0.34×10^{-8}
(α_2) K/G	-1.54×10^{-8}	$-1.57\times^{-8}$	-2.23×10^{-8}	-2.26×10^{-8}

These slight differences are due to contributions from the coefficients A_4 and A_5 which in contrast to A_3 are not proportional to α_J. We also remark that the anisotropy of Au:Yb does not depart significantly from what is predicted by the calculation; see Fig. 2. Therefore covalent mixing does not make a large contribution to the anisotropy of the resistivity. While covalent mixing is important in Au:Yb to account for the temperature dependence of the resistivity[19] and the very large isotropic magnetoresistance relative to that of alloys with other rare earths,[9] it does not appear very important for anisotropic transport properties; i.e., anisotropy of the magnetoresistance and Hall effect.[3]

The isotropic magnetoresistance must be discussed separately for alloys with non-S-state impurities and with Gd. For non-S-state impurities the expression for the isotropic magnetoresistance [see Eqs. (3.9), (3.12), and (3.19)] is fairly complicated and includes several terms having the same

TABLE IV. Calculated and experimental values of the quadrupole scattering coefficient a for a series of Ag:$\mathscr{R}$ and Au:$\mathscr{R}$ alloys. The concentrations of rare-earth impurities are also listed. The calculated values were arrived at by using Eq. (3.27) with the phase shifts given in Table I and the parameter A_3, A_4, and A_5 in Table V.

	C (at. %)	$a\times10^3$ calculated	$a\times10^3$ experiment
Ag:Dy	1.06	0.98	0.96
Ag:Ho	0.96	0.38	0.38
Ag:Er	1.95	−0.32	−1.25
Ag:Tm	2	−1.44	−2.55
Au:Tb	0.98	0.75	1.02
Au:Dy	1.4	0.51	0.51
Au:Ho	1	0.23	0.19
Au:Er	0.91	−0.11	−0.23
Au:Tm	0.86	−0.65	−1.36
Au:Yb	1.5	−2.24	−2.31

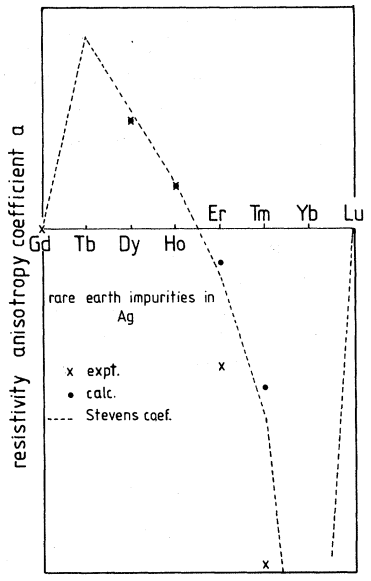

FIG. 2. Variation of the calculated and experimental values of the resistivity anisotropy coefficient a [see Eq. (4.5)] for heavy rare-earth impurities in Ag.

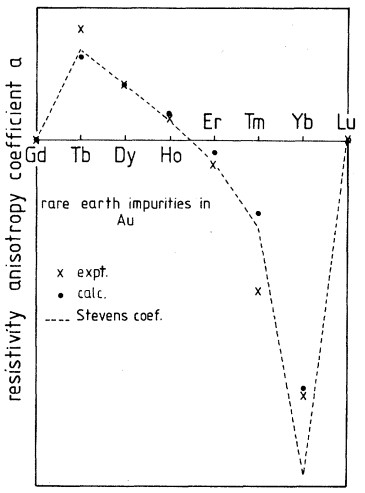

FIG. 3. Variation of the calculated and experimental values of the resistivity anisotropy coefficient a [see Eq. (4.5)] for heavy rare-earth impurities in Au.

order of magnitude. This has been discussed in detail by Ousset *et al.*[9] For crystal-field-split $4f$ levels there are negative and positive contributions to ρ^{iso} that vary differently as a function of the field. The combination of these terms can explain that the experimental isotropic magnetoresistance is generally negative at low field and becomes positive above about 100 kG. However, Ousset *et al.*[9] have been unable to obtain a quantitative fit of their experimental curves by using our theoretical expressions with the phase shifts of Table II. This is probably because the total effect is the sum of nearly canceling terms, so that small errors in the coefficients of these terms can significantly change the final result. This may also be due to the weakness of the isotropic magnetoresistance which, for non-S-state ions, is much smaller than the anisotropic magnetoresistance and therefore difficult to extract accurately from experimental data. For these reasons we have left out the quantitative interpretation of the isotropic part of the magnetoresistance of alloys containing non-S-state impurities.

In contrast, the interpretation of the isotropic magnetoresistance of Ag:Gd and Au:Gd alloys does not raise such difficulties. Its theoretical expression is written as [see Eqs. (3.9), (3.12), (3.19), and (3.21)]:

$$\frac{\Delta\rho^{iso}}{\rho_0} = -\gamma(\langle J_Z\rangle)^2 - \beta|\langle J_Z\rangle|\left[\coth\frac{\alpha}{2} - \frac{\alpha/2}{\sinh^2\alpha/2}\right], \tag{4.6}$$

where

$$\alpha = \frac{g_J\mu_B H}{k_B T}$$

and β,γ are given by Eqs. (3.23) and (3.24).

The experimental results[9] show a negative magnetoresistance in excellent agreement with the preceding expression. When one uses the phase shifts derived above (see Table II) and calculates β and γ from Eqs. (3.23) and (3.24), the best agreement is obtained by taking a value of A_0 reduced with respect to its atomic value by a factor of 2.12 for Ag:Gd and 2.56 for Au:Gd.

Finally, we apply the model to the Hall effect. The theoretical expression of the contribution from skew scattering to the Hall effect at high temperatures can be written as [see Eq. (3.29)]:

TABLE V. Effective values of the $4f$-$5d$ parameters giving the best fit for the magnetotransport properties and the corresponding atomic values. The atomic values are derived from atomic spectra; see Refs. 20 and 21. As the $4f$-$5d$ integrals for $\mathscr{R}$ II ions with one $5d$ and one $6s$ outer electrons do not change significantly throughout the heavy $\mathscr{R}$ series, we take the values for Dy II ($4f^9 5d\ 6s$ configuration) (Ref. 21).

	Ag:$\mathscr{R}$		Au:$\mathscr{R}$	
	Atomic value (cm^{-1})	Effective value (cm^{-1})	Atomic value (cm^{-1})	Effective value (cm^{-1})
A_0	1719	811.8	1719	672
A_1	58.8	35.1	58.8	33.2
A_2	96.97	57.6	96.97	37.9
A_3	1890	1122.3	1890	834.74
A_4	880	522.9	880	388.6
A_5	1444	857.7	1444	637.7

$$\frac{\rho_{xy}^{E}}{\rho_0}=[\alpha_1 g_J(2-g_J)J(J+1)$$

$$+\alpha_2 g_J(g_J-1)J(J+1)]\frac{H}{T}\ , \qquad (4.7)$$

where the two terms in the square brackets arise from $4f$-$5d$ orbital exchange and spin exchange together with spin-orbit splitting of the $5d$ VBS. The expressions for α_1 and α_2 are given by Eqs. (3.30) and (3.31). According to Fert and Friederich,[3] the experimental results throughout the $\mathscr{R}$ series can be accounted for by Eq. (4.7) with

$$\alpha_1=0.43\times10^{-8}\ \text{K/G}\ ,$$

$$\alpha_2=-1.57\times10^{-8}\ \text{K/G}\ \text{ for Ag:}\mathscr{R}\ ,$$

and

$$\alpha_1=0.34\times10^{-8}\ \text{K/G}\ ,$$

$$\alpha_2=-2.26\times10^{-8}\ \text{K/G}\ \text{ for Au:}\mathscr{R}\ .$$

Good agreement, for each alloy system, is obtained by inserting in Eqs. (3.30) and (3.31) the values of the phase shifts determined above (see Table II), the values of A_0 already used in the interpretation of the magnetoresistance, and a value of A_1 reduced with respect to its atomic value by nearly the same proportion as A_0. The experimental and calculated values of α_1 and α_2 are compared in Table III and the effective and atomic values of A_0 and A_1 are listed in Table V.

In summary, our theoretical model allows us to consistently interpret a large number of transport data: residual resistivity, thermoelectric power, isotropic magnetoresistance of alloys with Gd, anisotropic magnetoresistance of alloys with non-S-state impurities, and the spin and orbital terms of the skew scattering contribution to the Hall effect. Good agreement is obtained by assuming that the $4f$-$5d$ Slater-type integrals are reduced with respect to their atomic values by a factor of about 2. This reduction results from the wider radial extension of the $5d$ wave functions in the VBS relative to the $4f$ wave function. We also find that a relatively small spin-orbit splitting of the $5d$ VBS explains the experimental observation that alloys with Gd exhibit a significant skew scattering but no measurable anisotropy of the resistivity. If one uses the relation

$$\eta_{3/2}-\eta_{1/2}=\frac{3}{2}\frac{\lambda_{\text{eff}}}{\Delta}\sin^2\eta_{t_{2g}}$$

$$+\frac{3}{4}\frac{\lambda_{\text{eff}}^2}{\Delta^2}\sin^3\eta_{t_{2g}}\cos\eta_{t_{2g}}\ , \qquad (4.8)$$

our result on $(\eta_{3/2}-\eta_{1/2})$ corresponds to

$$\lambda_{\text{eff}}\simeq0.216\ \text{ in Ag}\ ,$$

$$\lambda_{\text{eff}}\simeq0.64\ \text{ in Au}\ .$$

These effective values of the spin-orbit constant of the $5d$ electrons are larger than the atomic ones, as expected by the theory of Yafet.[22] The enhancement factor of λ appears to be about 2 in Ag host. In Au it should be about 6, which is surprisingly large. This could be due to the additional effect of the spin-orbit coupling of the Au host.

In a previous publication,[2] a first version of our model was presented without spin-orbit splitting of the VBS. The introduction of the spin-orbit splitting in the present model allows us to account for the spin component of the skew scattering, the α_2 term. Also the general agreement with experiment is better. In particular, in the previous model, it was necessary to reduce the $4f$-$5d$ *exchange* integrals with respect to their atomic values but not the *direct* integrals. In the present model all the $4f$-$5d$ integrals have to be reduced in the same way, which seems more reasonable. Also, as we shall see in the next paragraph, the present model gives also a better interpretation of the EPR data.

In the Appendix we develop another version of our model with spin-orbit splitting but *without* crystal-field splitting. The agreement with experiment is definitely worse which justifies *a posteriori* our model with the large crystal-field splitting, i.e., t_{2g} only VBS.

B. Electron paramagnetic resonance

We have calculated $\Delta H/\Delta T$ and the g shift by using in Eqs. (3.41) and (3.48) the values of the phase shifts, VBS width, and $4f$-$5d$ coefficients determined from the transport properties. The calculated values are listed in Table VI together with the experimental values for those alloys for which experimental data exist, except Au:Yb for which additional effects coming from covalent mixing should be taken into account.[23] It turns out that the calculated values of $\Delta H/\Delta T$, and to a lesser extent those of Δg, are too small. These results indicate that the $5d$ VBS is not sufficient to account for the magntiudes observed experimentally and that another contribution is present. In fact, this model only takes into account the exchange scattering in the $l=2$ channel and ignore any exchange scattering in other channels, in particular, in the $l=0$ channel. We will now show that add-

TABLE VI. Experimental and calculated EPR linewidths and g shifts. The d contributions have been calculated with the parameters derived from the magnetotransport properties, and the s contributions with $J_s=0.075$ eV.

	$\left[\frac{\Delta H}{\Delta T}\right]_d$ G/K	$\left[\frac{\Delta H}{\Delta T}\right]_s$ G/K	$\left[\frac{\Delta H}{\Delta T}\right]_{\text{tot}}$ G/K	$\left[\frac{\Delta H}{\Delta T}\right]_{\text{expt}}$ G/K	$(\Delta g)_d$	$(\Delta g)_s$	$(\Delta g)_{\text{tot}}$	$(\Delta g)_{\text{expt}}$
Au:Gd	2.49	2.96	5.45	7±2[a]	0.023	0.011	0.034	0.05±0.01[a]
								0.045[b]
Au:Er	0.37	1.12	1.49	2.7±0.05[c]	0.033	0.013	0.046	
				2[d]				0[d]
Ag:Er	3.69	1.12	4.81	10.5±1.5[e]	0.056	0.013	0.069	0.05+0.4[e]
				7±1[f]				
Ag:Dy	9.62	2.8	12.42	18.5±2[g]	0.085	0.021	0.106	
				23±5[f]				0.07±0.05[f]
Ag:Gd	11	2.96	13.96	19±7[f]	0.04	0.011	0.051	0.08±0.01[f]

[a]Reference 26.
[b]Reference 27.
[c]Reference 28.
[d]Reference 29.
[e]Reference 30.
[f]Reference 31.
[g]Reference 32.

ing and $l=0$ exchange scattering allows us to improve the agreement with EPR data but does not significantly alter the agreement already found for the transport data.

We assume an additional exchange interaction of the form

$$H_s=J_s\cdot N^{-1}\vec{s}\cdot\vec{S}\delta(r)\ . \tag{4.9}$$

There is no interference between exchange scattering in the $l=0$ and $l=2$ channels so that H_s, Eq. (4.9), provides an independent contribution to $\Delta H/\Delta T$. For a doublet ground state with gyromagnetic factor g, this contribution is given by the classical expression[24]

$$\left[\frac{\Delta H}{\Delta T}\right]_s=\frac{\pi g k_B}{\mu_B}\left[\frac{(g_J-1)J_s n(E_F)}{g_J}\right]^2\ . \tag{4.10}$$

The contribution to the g shift is[23]

$$(\Delta g)_s=g\left[\frac{g_J-1}{g_J}\right]J_s n(E_F)\ . \tag{4.11}$$

Finally, the isotropic spin exchange H_s contributes to the isotropic magnetoresistance but not to the anisotropic magnetoresistance or to the Hall effect. A straightforward calculation gives us the contribution to the isotropic magnetoresistance as

$$\frac{\Delta\rho^{\text{iso}}}{\rho_0}=-\frac{D}{\rho_0}[\pi(g_J-1)J_s n(E_F)]^2 \times\left[\frac{D}{4\rho_0}\sin^2\eta_0\cos^2\eta_0(\langle J_Z\rangle)^2+\tfrac{1}{8}(\langle\vec{J}\cdot W\vec{J}\rangle_{H=0}-\langle\vec{J}\cdot W\vec{J}\rangle_H)\right]\ . \tag{4.12}$$

By taking a value of $J_s=0.075$ (Ref. 24) and adding the s and d contributions, we obtain for $\Delta H/\Delta T$ and Δg good agreement with the experimental results; see Table VI. The s and d contributions are of the same order of magnitude. We have also calculated the s contribution to $\Delta\rho^{\text{iso}}$, Eq. (4.12), and find it is small; about 10% of the d contribution, and therefore it is not significant for the transport properties.

We conclude that the contribution from s exchange scattering can be neglected for the magnetotransport properties but is significant for the EPR properties. In our analysis about one-half of the linewidth arises from the s contribution. Another difference between EPR and magnetotransport is that the EPR is less sensitive to the anisotropy of the k-f interaction. Whereas the anisotropy is essential to explain some magnetotransport properties, e.g., the anisotropy of the resistivity results from quadrupole scattering, the term α_1

of the Hall effect from orbital exchange and the term α_2 from the spin-orbit coupling of the d electrons, the EPR depends mainly on the isotropic parts (s and d) of the k-f exchange interaction. For example, we find that the contribution from orbital exchange to $(\Delta H/\Delta T)_d$ for Dy or Er impurities does not exceed 30% of the contribution from spin exchange.

As discussed in the Appendix, we also tried to interpret the EPR data within a 5d VBS model *without* crystal-field splitting of the d states. Again we fix the phase shifts and the 4f-5d parameters to fit the magnetotransport data and then calculate $(\Delta H/\Delta T)_d$ and $(\Delta g)_d$ with these values of the parameters. We find that, for all the alloys, $(\Delta H/\Delta T)_d$ is smaller than the t_{2g} VBS model values and thus much smaller than the experimental values. By using the model of Huang Liu *et al.*, which is similar to the 5d VBS model but without spin-orbit coupling,[25] and the 4f-5d parameters derived from magnetotransport data one also obtains values of $(\Delta H/\Delta T)_d$ much smaller than the experimental ones. This gives us an additional reason to prefer the t_{2g} VBS model.

V. DISCUSSION OF RESULTS AND CONCLUSIONS

We have found that the model for the local-moment—conduction-electron interaction based on a virtual bound state description for the rare-earth's outer 5d electron and on *all* components of the 4f-5d Coulomb interaction is able to provide a consistent description of a large amount of transport and resonance data. In the present analysis we included the spin-orbit coupling of the conduction electrons so that the model can account for the spin contribution to the extraordinary Hall effect α_2, which is most evident for Gd^{3+} as the orbital contribution α_1 is zero for S-state ions. We are able to obtain good fits to all the data by choosing similar values of the screening charges and 4f-5d interaction parameters for the silver- and gold-based alloys, by using the linewidth Δ of the VBS in silver found from optical data ($\Delta=0.45$ eV) and by adjusting Δ for gold-based alloys to give the correct magnitude of the thermoelectric power. This leads to a larger value of the linewidth ($\Delta=0.6$ eV) in gold, which also provides good agreement for all data depending on Δ. It is generally admitted that the d VBS of a transition-metal or rare-earth impurity in gold should be repelled upwards by the presence of the 5d level of Au close to the Fermi level. Our results indicate that the 5d VBS of rare-earth impurities in gold is not only repelled but also broadened (stronger mixing than in silver), so that *in toto* the VBS occupancy is not very different in gold and silver. The stronger mixing in gold can be explained by the strong d character of the conduction band at the Fermi level, which is also related to the proximity of the 5d level of gold to the Fermi level.

Of the two models used in our analysis the one with the crystal-field-split 5d-t_{2g} VBS produced a slightly better fit to the transport properties than the full 5d VBS scheme. However, at least for the silver-based alloys, the clear advantage of the crystal-field-split VBS is that the spin-orbit coupling parameter $\lambda\cong 0.22$ eV is much closer to the atomic value for 5d electrons. For the gold-based alloys the parameter λ in both schemes is much larger than the atomic 5d value, albeit the λ for the 5d-t_{2g} VBS is closer to λ_{5d}. This increase may be due to the additional contribution to λ from the host conduction electrons in gold. Another reason for our preference of the crystal-field-split VBS is that it allows a better interpretation of the EPR data.

The major improvement over previous analyses of the transport and EPR data for rare-earth impurities is that compared to their atomic values all the 4f-5d interaction parameters need about the *same* reduction factor (1.9 to 2.5) to fit all the data. This reduction for impurities in metals is due to the differential expansions of the 5d orbital relative to the 4f shell. It arises from the screening by the conduction electrons of the nuclear charge. The screening by conduction electrons is more effective for the 5d electrons and therefore this orbital expands more in a metal than the 4f shell.

The reason for the uniformity in the reduction factor is only partially due to our inclusion of the spin-orbit coupling and the p-wave phase shift of the conduction electrons. It is mainly due to our using new spectroscopic data to determine the atomic values of the 4f-5d interaction parameters. From our analysis we find that for non-S-state ions the multipole, e.g., quadrupole, part of the k-f interaction A_3, is comparable in size to the bilinear spin interaction A_0. For the conduction electrons to perceive the multipole components of this interaction it is necessary to consider their resonant mixing with the rare-earth impurities's 5d electrons, i.e., the virtual bound state. Therefore those early analyses which neglected the higher-rank

components of the k-f interaction and the VBS character of the conduction electrons about the impurity (considering only isotropic spin exchange between the local moment and conduction electron in plane-wave states) are incomplete.

For Gd impurities a small anisotropy on the k-f interaction still exists due to the spin-orbit splitting of the $5d$ VBS. We find that this splitting is relatively small so that the anisotropy effects depending linearly on λ, e.g., the extraordinary Hall effect, are larger than higher-order terms, e.g., the anisotropy of the resistivity. Finally, the previous discrepancies between transport and EPR properties based on the VBS model have been resolved by our adding a necessary factor of 5 reduction to the previously calculated linewidth.

Aside from providing a unified description of diverse physical properties of rare-earth local moments in metals, our study will be useful in the future in at least two areas. First in estimating the crystal-field splitting of S state ions due to the simultaneous effects on outer electrons of the crystal-field, spin-orbit coupling and the resonant mixing with conduction electrons. Second, when one considers two rare-earths, the resonant mixing of the outer d electrons with the conduction electrons of the host metal couples the ions. By including the higher-rank multipole $4f$-$5d$ interactions one can find the magnitude of the multipolar pair interactions mediated by the conduction electrons.

ACKNOWLEDGMENTS

We want to thank Professor N. L. Huang-Liu and Professor R. L. Orbach for valuable communications which led to our resolving the numerical differences in our expressions for the linewidths. This work was supported in part by the National Science Foundation under Grant No. DMR78-25008 and the Centre National de la Recherche Scientifique under the United States—France Cooperative Science Program.

APPENDIX: EVALUATION OF THE MAGNETOTRANSPORT COEFFICIENTS FOR A $5d$ STATE WITH SPIN-ORBIT COUPLING

To test the validity of the assumption that only t_{2g} states are occupied, one can consider a different limit, namely to take into account the full $5d$ level with spin-orbit coupling. In this case the states are given by

$$|\vec{k}^{\pm}\sigma\rangle=\sum_{j=3/2}^{5/2}\sum_{m_j}C^{\pm}_{jm_j}(\vec{k})\,|jm_j\rangle\ , \tag{A1}$$

where

$$C^{\pm}_{jm_j}=e^{\pm i\eta_j}\sin\eta_j\frac{\langle d\,|\,V_0\,|\,k\rangle}{\Delta}\sum_m Y_{2m}(\Omega_{\vec{k}})\langle jm_j\,|\,m\sigma\rangle\ ,$$

and $j=l\pm\frac{1}{2}=\frac{3}{2},\frac{5}{2}$ for a d electron.

Consequently the T matrix elements are given by

$$T^{(Q)}_{\vec{k}\sigma\to\vec{k}'\sigma'}=-\frac{4}{N}\left[\frac{\delta_{\sigma\sigma'}}{4\pi}e^{i\eta_0}\sin\eta_0+\delta_{\sigma\sigma'}e^{i\eta_1}\sin\eta_1\right.$$
$$\times\sum_m Y^*_{1m}(\Omega_{\vec{k}})Y_{1m}(\Omega_{\vec{k}'})$$
$$\left.+\sum_j e^{i\eta_j}\sin\eta_j\sum_{\substack{m\\m'}}{}'\langle 2\tfrac{1}{2}m'\sigma'\,|\,jm_j\rangle\langle jm_j\,|\,2\tfrac{1}{2}m\sigma\rangle Y_{2m}(\Omega_{\vec{k}})Y^*_{2m'}(\Omega_{\vec{k}'})\right]\ , \tag{A2}$$

where the prime over the summation symbol denotes

$$m_j=m+\sigma\ ,$$
$$m'_j=m'+\sigma'\ ,$$

and

$$\langle jm_j \mid 2\tfrac{1}{2} m\sigma\rangle = (-1)^{2-(1/2)+m_j}\sqrt{2j+1}\begin{Bmatrix} j & 2 & \frac{1}{2} \\ -m_j & m & \sigma \end{Bmatrix}$$

$$= \delta_{j,5/2}\frac{1}{\sqrt{5}}(\tfrac{5}{2}+2\sigma m_j)^{1/2} - \delta_{j,3/2}\frac{2\sigma}{\sqrt{5}}(\tfrac{5}{2}-2\sigma m_j)^{1/2}\,, \tag{A3}$$

$$dT^{(1)}_{\vec{k}\sigma\to\vec{k}'\sigma'} = \frac{4}{N\Delta}\sum_{jj'}\exp[i(\eta_j+\eta'_j)]\sin\eta_j\sin\eta'_j \times \sum_{\substack{m\\ m'}}{}' \langle 2\tfrac{1}{2} m'\sigma' \mid j'm'_j\rangle\langle j'm'_j \mid v \mid jm_j\rangle\langle jm_j \mid 2\tfrac{1}{2} m\sigma\rangle Y^*_{2m'}(\Omega_{\vec{k}'})Y_{2m}(\Omega_{\vec{k}})\,, \tag{A4}$$

where

$$m_j = m+\sigma\,,$$
$$m'_j = m'+\sigma'\,,$$

$$dT^{(2)}_{\vec{k}\sigma\to\vec{k}'\sigma'} = \frac{4}{N\Delta}\sum_{jj'}\exp[i(\eta_j+n'_j)]\sin\eta_j\sin\eta'_j \times \sum_{\substack{m\\ m'}}{}' \langle 2\tfrac{1}{2} m'\sigma' \mid j'm'_j\rangle\langle j'm'_j \mid vGv \mid jm_j\rangle\langle jm_j \mid 2\tfrac{1}{2} m\sigma\rangle Y^*_{2m'}(\Omega_{\vec{k}'})Y_{2m}(\Omega_{\vec{k}})\,, \tag{A5}$$

where

$$m_j = m+\sigma\,,$$
$$m'_j = m'+\sigma'\,,$$

and $\langle j'm'_j \mid vGv \mid jm_j\rangle$ is given by Eq. (2.19).

The matrix element of the perturbation v is the following:

$$\begin{aligned}\langle j'm_j \mid v \mid jm_j\rangle = m_j\langle J_Z\rangle &\left[\left(-\frac{A_0\mathscr{P}_0}{5}-\frac{4}{5}A_1\mathscr{P}_1-\frac{6}{\sqrt{5}}A_2\mathscr{P}_2\right)\delta_{j,5/2}\delta_{j',5/2}\right.\\ &\left.+\left(\frac{A_0\mathscr{P}_0}{5}-\frac{6}{5}A_1\mathscr{P}_1+\frac{21}{\sqrt{5}}A_2\mathscr{P}_2\right)\delta_{j,3/2}\delta_{j',3/2}\right]\\ &+\langle J_Z\rangle\left(\frac{25}{4}-m_j^2\right)^{1/2}\left(\frac{A_0\mathscr{P}_0}{5}-\frac{A_1\mathscr{P}_1}{5}-\frac{21}{4\sqrt{5}}A_2\mathscr{P}_2\right)\delta_{j\neq j'}\\ &+\langle O_0^2\rangle\left[\left(3m_j^2-\frac{35}{4}\right)\left(\frac{3}{2\sqrt{5}}A_3\mathscr{P}_3-\frac{7}{\sqrt{5}}A_4\mathscr{P}_4+\frac{1}{3\sqrt{5}}A_5\mathscr{P}_5\right)\delta_{j,5/2}\delta_{j',5/2}\right.\\ &\left.+\left(m_j^2-\frac{5}{4}\right)\left(\frac{21}{2\sqrt{5}}A_3\mathscr{P}_3+\frac{3}{\sqrt{5}}A_4\mathscr{P}_4-\frac{7}{\sqrt{5}}A_5\mathscr{P}_5\right)\delta_{j,3/2}\delta_{j',3/2}\right.\\ &\left.+m_j\left(\frac{25}{4}-m_j^2\right)^{1/2}\left(\frac{3}{\sqrt{5}}A_3\mathscr{P}_3+\frac{3}{\sqrt{5}}A_4\mathscr{P}_4-\frac{4}{3\sqrt{5}}A_5\mathscr{P}_5\right)\delta_{j\neq j'}\right]\,.\end{aligned} \tag{A6}$$

By using these expressions and the Wigner-Eckart theorem (to obtain the elements with $m_{j'} \neq m_j$), we obtain expressions for the resistivity similar to those of Sec. III. In particular, the expressions for the magnetotransport properties we are going to compare with experimental data are as follows:

1. Impurity Resistivity

$$\rho_0 = \frac{D}{2}[\sin^2(\eta_0-\eta_1)+\sin^2(\eta_{5/2}-\eta_1)+\sin^2(\eta_{3/2}-\eta_1)+2\sin^2\eta_{5/2}+\sin^2\eta_{3/2}] , \tag{A7}$$

where D is given by Eq. (3.6).

2. Hall Resistivity

$$\frac{\rho_{xy}^E}{\rho_0} = [\alpha_1 g_J(2-g_J)J(J+1)+\alpha_2 g_J(g_J-1)J(J+1)]\frac{H}{T} , \tag{A8}$$

where

$$\alpha_1 = \frac{7D\mu_B A_1 \sin\eta_1}{25\Delta k_B \rho_0}[\,2\sin^2\eta_{5/2}\sin(2\eta_{5/2}-\eta_1)+\tfrac{9}{7}\sin^2\eta_{3/2}\sin(2\eta_{3/2}-\eta_1) + \tfrac{2}{7}\sin\eta_{3/2}\sin\eta_{5/2}\sin(\eta_{5/2}+\eta_{3/2}-\eta_1)] \tag{A9}$$

and

$$\alpha_2 = \frac{7D\mu_B A_0 \sin\eta_1}{50\Delta k_B \rho_0}[\,\sin^2\eta_{5/2}\sin(2\eta_{5/2}-\eta_1)-\tfrac{3}{7}\sin^2\eta_{3/2}\sin(2\eta_{3/2}-\eta_1) - \tfrac{4}{7}\sin\eta_{3/2}\sin\eta_{5/2}\sin(\eta_{5/2}+\eta_{3/2}-\eta_1)] . \tag{A10}$$

3. Anisotropic Magnetoresistivity

$$\frac{\rho_{\parallel}-\rho_{\perp}}{\rho_0} = a\left[\langle\langle J_Z^2\rangle\rangle - \frac{J(J+1)}{3}\right] , \tag{A11}$$

where

$$a = \frac{63\sqrt{6}D}{200\Delta\rho_0}\{\,8\tilde{B}_4\sin^2\eta_{5/2}[\tfrac{2}{7}\sin\eta_{5/2}\cos\eta_{5/2}+\tfrac{1}{10}\sin\eta_1\cos(2\eta_{5/2}-\eta_1)] + \tfrac{2}{3}\tilde{B}_6\sin^2\eta_{3/2}[\tfrac{2}{7}\sin\eta_{3/2}\cos\eta_{3/2}+\tfrac{1}{10}\sin\eta_1\cos(2\eta_{3/2}-\eta_1)] + \tilde{B}_5\sin\eta_{3/2}\sin\eta_{5/2}[\tfrac{2}{7}\sin\eta_{3/2}\cos\eta_{5/2}+\tfrac{2}{7}\sin\eta_{5/2}\cos\eta_{3/2}+\tfrac{2}{10}\sin\eta_1\cos(\eta_{3/2}+\eta_{5/2}-\eta_1)]\} , \tag{A12}$$

$$\tilde{B}_4 = \tfrac{3}{2}\mathscr{P}_3 A_3 - A_4\mathscr{P}_4 - \tfrac{1}{3}A_5\mathscr{P}_5 ,$$

$$\tilde{B}_5 = 3A_3\mathscr{P}_3 + 3A_4\mathscr{P}_4 - \tfrac{4}{3}A_5\mathscr{P}_5 ,$$

$$\tilde{B}_6 = \tfrac{21}{2}A_3\mathscr{P}_3 + 3A_4\mathscr{P}_4 - 7A_5\mathscr{P}_5 .$$

For Gd^{3+} we must include higher-order terms in the expression of $\rho_{||}-\rho_{\perp}$ since this first contribution is zero, and we obtain

$$\left[\frac{\rho_{||}-\rho_{\perp}}{\rho_0}\right]_{\mathrm{Gd}} = \frac{3\sqrt{6}DA_0^2}{80\Delta^2\rho_0}$$

$$\times\Big[\langle\vec{J}\cdot W\vec{J}\rangle(\tfrac{7}{2}\sin^4\eta_{5/2}+\sin^4\eta_{3/2}+8\sin^2\eta_{3/2}\sin^2\eta_{5/2})$$

$$+\tfrac{12}{25}[\langle J_Z^2\rangle-\tfrac{1}{3}J(J+1)]\{8\sin^4\eta_{5/2}\cos2\eta_{5/2}+4\sin^4\eta_{3/2}\cos2\eta_{3/2}$$

$$-8\sin\eta_{3/2}\sin^3\eta_{5/2}\cos(\eta_{3/2}+\eta_{5/2})-2\sin\eta_{5/2}\sin^3\eta_{3/2}\cos(\eta_{3/2}+\eta_{5/2})$$

$$+35[\sin^2\eta_{3/2}\sin^2\eta_{5/2}\cos2\eta_{3/2}+\sin^3\eta_{3/2}\sin\eta_{5/2}\cos(\eta_{3/2}+\eta_{5/2})]$$

$$-\tfrac{105}{2}[\sin^2\eta_{5/2}\sin^2\eta_{3/2}\cos2\eta_{5/2}+\sin^3\eta_{5/2}\sin\eta_{3/2}\cos(\eta_{3/2}+\eta_{5/2})]\}$$

$$-\frac{28D}{25\rho_0}\langle J_Z\rangle^2\{\sin^2\eta_{5/2}[\tfrac{2}{7}\sin\eta_{5/2}\cos\eta_{5/2}+\tfrac{1}{10}\sin\eta_1\cos(2\eta_{5/2}-\eta_1)]$$

$$+\sin^2\eta_{3/2}[\tfrac{2}{7}\sin\eta_{3/2}\cos\eta_{3/2}+\tfrac{1}{10}\sin\eta_1\cos(2\eta_{3/2}-\eta_1)]$$

$$-\sin\eta_{3/2}\sin\eta_{5/2}[\tfrac{2}{7}\sin\eta_{3/2}\cos\eta_{5/2}+\tfrac{2}{7}\sin\eta_{5/2}\cos\eta_{3/2}$$

$$+\tfrac{1}{5}\sin\eta_1\cos(\eta_{3/2}+\eta_{5/2}-\eta_1)]\}$$

$$\times\{7\sin^2\eta_{5/2}[\cos\eta_{5/2}\sin\eta_{5/2}-\tfrac{1}{5}\sin\eta_1\cos(2\eta_{5/2}-\eta_1)]$$

$$-2\sin^2\eta_{3/2}[\sin\eta_{3/2}\cos\eta_{3/2}-\tfrac{1}{5}\sin\eta_1\cos(2\eta_{3/2}-\eta_1)]$$

$$-8\sin\eta_{3/2}\sin\eta_{5/2}[\sin\eta_{5/2}\cos\eta_{3/2}+\sin\eta_{3/2}\cos\eta_{5/2}-\tfrac{2}{5}\sin\eta_1\cos(\eta_{5/2}+\eta_{3/2}-\eta_1)]\}\Big]\,. \tag{A13}$$

TABLE VII. Phase shifts giving the best agreement with experimental results (see Table X) and corresponding screening charges.

	Ag:$\mathscr{R}$		Au:$\mathscr{R}$	
	η_l	Z_l	η_l	Z_l
$l=0$	1.56	0.99	1.56	0.99
$l=1$	0.04	0.08	0.13	0.25
$\tilde{j}=\frac{3}{2}$	0.52	0.66	0.42	0.53
$\tilde{j}=\frac{5}{2}$	0.14	0.27	0.12	0.23

TABLE VIII. Effective values of the $4f$-$5d$ parameters giving the best fit for the magnetotransport properties compared with corresponding atomic values.

	Ag:$\mathscr{R}$ Effective value (cm^{-1})	Au:$\mathscr{R}$ Effective value (cm^{-1})	Atomic value (cm^{-1})
A_0	1078.2	987.6	1719
A_1	54.9	27.6	58.8
A_2	87.3	79.96	96.97
A_3	1475	986.4	1890
A_4	686.7	459.6	880
A_5	1126.8	753.6	1444

4. *Isotropic Magnetoresistivity*

$$\left[\frac{\Delta\rho^{\text{iso}}}{\rho_0}\right]_{\text{Gd}} = \frac{DA_0^2}{50\Delta^2\rho_0}(\langle \vec{J}\cdot W\vec{J}\rangle_H - \langle \vec{J}\cdot W\vec{J}\rangle_0)(\tfrac{35}{4}\sin^4\eta_{5/2}+\tfrac{5}{2}\sin^4\eta_{3/2}+20\sin^2\eta_{3/2}\sin^2\eta_{5/2})$$
$$-\frac{D^2A_0^2\langle J_Z\rangle^2}{100\Delta^2\rho_0^2}\{-7\sin^2\eta_{5/2}[\cos\eta_{5/2}\sin\eta_{5/2}-\tfrac{1}{5}\sin\eta_1\cos(2\eta_{5/2}-\eta_1)]$$
$$-8\sin\eta_{3/2}\sin\eta_{5/2}[\sin\eta_{5/2}\cos\eta_{3/2}+\sin\eta_{3/2}\cos\eta_{5/2}-\tfrac{2}{5}\sin\eta_1\cos(\eta_{5/2}+\eta_{3/2}-\eta_1)]\}^2 . \tag{A14}$$

By following the procedure described in Sec. IV we obtain a set of parameters η's and A's (see Tables VII and VIII) which give us the results shown in Tables IX and X.

For the EPR properties we notice that by using Eqs. (3.40), (3.34), and the expression derived above for the resistivity, we obtain for the linewidth (d contribution),

$$\frac{\Delta H}{\Delta T} = \frac{k_B g}{\pi\mu_B\Delta^2 g_J^2}(35\tilde{B}_1^2\sin^4\eta_{5/2}+10\tilde{B}_3^2\sin^4\eta_{3/2}+80\tilde{B}_2^2\sin^2\eta_{3/2}\sin^2\eta_{5/2}) , \tag{A15}$$

where

TABLE IX. Compared experimental and calculated transport properties of Ag:$\mathscr{R}$ and Au:$\mathscr{R}$ alloys. The first five lines have been calculated with the phase shifts of Table VII and, for the TEP, with the values of Δ indicated in the text. The skew scattering coefficients α_1 and α_2 have been calculated with the same parameters and the values of A_0 and A_1 given in Table VIII.

	Ag host		Au host	
	Calc.	Expt.	Calc.	Expt.
ρ_0 ($\mu\Omega$ cm/at. %)	6.5	5.2–6	5.46	7
$A\equiv S/T$ (V/K^2)	1.54×10^{-8}	1.79×10^{-8}	0.72×10^{-8}	1.1×10^{-8}
$\frac{\alpha_2}{\alpha_1}$	−3.62	−3.65	−6.75	−6.647
$\left[\alpha_2\Big/\left\lvert\frac{\Delta\rho^{\text{iso}}}{\rho_0}\right\rvert^{1/2}\right]^{\text{sat}}_{\text{Gd}}$ (K/G)	-1.29×10^{-7}	-1.28×10^{-7}	-3.5×10^{-7}	-3.57×10^{-7}
$\left\lvert\frac{\rho_\parallel-\rho_\perp}{\Delta\rho^{\text{iso}}}\right\rvert^{\text{sat}}_{\text{Gd}}$	0.04	0.04	0.05	0.04
α_1 (K/G)	0.437×10^{-8}	0.43×10^{-8}	0.327×10^{-8}	0.34×10^{-8}
α_2 (K/G)	-1.58×10^{-8}	-1.57×10^{-8}	-2.21×10^{-8}	-2.26×10^{-8}

TABLE X. Calculated and experimental values of the quadrupole scattering coefficient a for a series of Ag:$\mathscr{R}$ and Au:$\mathscr{R}$ alloys. The experimental concentrations are also listed.

	c (at. %)	$a\times10^3$ Calculated	$a\times10^3$ Experiment
Ag:Dy	1.06	0.84	0.96
Ag:Ho	0.96	0.02	0.38
Ag:Er	1.95	−0.95	−1.25
Ag:Tm	2	−2.67	−2.55
Au:Tb	0.98	0.51	1.02
Au:Dy	1.4	0.28	0.51
Au:Ho	1	0.06	0.19
Au:Er	0.91	−0.20	−0.23
Au:Tm	0.86	−0.94	−1.36
Au:Yb	1.5	−2.94	−2.31

$$\tilde{B}_1=\frac{A_0\mathscr{P}_0}{5}+\tfrac{4}{5}A_1\mathscr{P}_1+\frac{6}{\sqrt{5}}A_3\mathscr{P}_3\ ,$$

$$\tilde{B}_2=\frac{A_0\mathscr{P}_0}{5}-\frac{A_1\mathscr{P}_1}{5}-\frac{21}{4\sqrt{5}}A_3\mathscr{P}_3\ ,$$

$$\tilde{B}_3=\frac{A_0\mathscr{P}_0}{5}-\tfrac{6}{5}A_1\mathscr{P}_1+\frac{21}{\sqrt{5}}A_3\mathscr{P}_3\ .$$

For the g shift, using Eqs. (3.44), (3.45), and (3.47), we obtain

$$\Delta g=\frac{A_0(g_J-1)g}{\pi g_J\Delta}\left(\tfrac{21}{5}\sin^2\eta_{5/2}-\tfrac{4}{5}\sin^2\eta_{3/2}+\tfrac{8}{5}\sin\eta_{5/2}\sin\eta_{3/2}\right)$$
$$+\frac{A_1(2-g_J)g}{\pi g_J\Delta}\left(\tfrac{84}{5}\sin^2\eta_{5/2}+\tfrac{24}{5}\sin^2\eta_{3/2}-\tfrac{8}{5}\sin\eta_{5/2}\sin\eta_{3/2}\right)\ . \tag{A16}$$

The values obtained for these two quantities when we use the parameters of Tables VII and VIII are given in Table XI.

TABLE XI. Experimental and calculated EPR linewidths and g shifts. The d contributions have been calculated with the parameters derived from the magnetotransport properties, and the s contributions with $J_s=0.075$ eV.

	$\left[\frac{\Delta H}{\Delta T}\right]_d$ G/K	$\left[\frac{\Delta H}{\Delta T}\right]_s$ G/K	$\left[\frac{\Delta H}{\Delta T}\right]_{\rm tot}$ G/K	$\left[\frac{\Delta H}{\Delta T}\right]_{\rm expt}$ G/K	$(\Delta g)_d$	$(\Delta g)_s$	$(\Delta g)_{\rm tot}$	$(\Delta g)_{\rm expt}$
Au:Gd	1.87	2.96	4.83	7±2[a]	0.0003	0.011	0.0113	0.05±0.1[a]
								0.045[b]
Au:Er	0.48	1.12	1.6	2.7±0.05[c]	0.008	0.013	0.021	
				2[d]				0[d]
Ag:Er	0.86	1.12	1.98	10.5±1.5[e]	0.029	0.013	0.042	0.05±0.04[e]
				7±1[f]				
Ag:Dy	4.4	2.8	7.2	18.5±2[g]	0.025	0.021	0.046	
				23±5[f]				0.07±0.05[f]
Ag:Gd	8.4	2.96	11.36	19±7[f]	−0.0004	0.011	0.0106	0.08±0.01[f]

[a]Reference 26.
[b]Reference 27.
[c]Reference 28.
[d]Reference 29.
[e]Reference 30.
[f]Reference 31.
[g]Reference 32.

*This work is based in part on a thesis submitted by G. Lacueva in partial fulfillment of the requirements for the Ph.D. at New York University.

[1]N. L. Huang-Liu, K. J. Ling, and R. Orbach, Phys. Rev. B 14, 4807 (1976).

[2]A. Fert and P. M. Levy, Phys. Rev. B 16, 5052 (1977).

[3]A. Fert and A. Friederich, Phys. Rev. B 13, 397 (1976).

[4]N. L. Huang-Liu and R. Orbach, Phys. Rev. B 17, 3701 (1978).

[5]A. Messiah, *Mécanique Quantique* (Duod, Paris, 1969).

[6]E. Daniel and J. Friedel, in *Proceedings of the Ninth International Conference on Low Temperature Physics,* edited by J. Daunt, P. Edward, F. Milford, and M. Yaqub (Plenum, New York, 1965).

[7]E. R. Callen and H. B. Callen, Phys. Rev. 129, 578 (1963).

[8]A. Fert and I. A. Campbell, J. Phys. F 6, 849 (1976); A. Fert, *ibid.* 3, 2126 (1973).

[9]J. C. Ousset, G. Carrere, J. P. Ulmet, S. Askenazy, G. Creuzet, and A. Fert, J. Magn. Magn. Mater. 24, 7 (1981).

[10]M. T. Beal-Monod and R. A. Weiner, Phys. Rev. 170, 552 (1968).

[11]A. Fert, R. Asomoza, D. Sanchez, D. Spanjaard, and A. Friederich, Phys. Rev. B 16, 5040 (1977).

[12]R. M. White, *Quantum Theory of Magnetism* (McGraw-Hill, New York, 1970).

[13]L. Dworin and A. Narath, Phys. Rev. Lett. 25, 1287 (1970).

[14]J. Bijvoet, A. J. Van Dam, and F. van Beek, Solid State Commun. 4, 455 (1966).

[15]L. R. Edwards and S. Legwold, J. Appl. Phys. 39, 120 (1968).

[16]F. F. Bekker and T. P. Hoogkamer, Physica 84B, 67 (1976).

[17]M. de Jong and F. F. Bekker, Physica B-C 86-88, 513 (1977).

[18]G. Lacueva, P. M. Levy, G. Creuzet, and A. Fert, Solid State Commun. 38, 551 (1981).

[19]A. P. Murani, J. Phys. C 2, S153 (1970).

[20]J. F. Wyart, Physica 61, 192 (1972).

[21]P. Camus and J. Sugar, Phys. Scr. 4, 257 (1971); and P. Camus, private communication.

[22]Y. Yafet, J. Appl. Phys. 39, 853 (1968).

[23]L. J. Tao, D. Davidov, R. Orbach, and E. P. Chock, Phys. Rev. 4, 5 (1971). A misprint in Eq. (1) has been corrected in later publications by the same group; see Ref. 28.

[24]To interpret the linewidth of Au:Er, Tao *et al.* (Ref. 23) took a larger value of J_s, i.e., $J_s=0.15$ eV, derived from hyperfine splitting. As the resulting contribution to $\Delta H/\Delta T$ is too large, they account for the experimental value of $\Delta H/\Delta T$ by adding a negative contribution ascribed to covalent mixing (CM). However, this reasoning is erroneous because s and CM. scattering act in different channels and therefore give independent positive contributions, $\Delta H/\Delta T \sim J_s^2+J_{CM}^2$ and not $(J_s+J_{CM})^2$. Therefore it is necessary to assume a smaller value of J_s to explain the data.

[25]In Eq. (17) of Ref. (1) a numerical correction factor is needed. The equation should be divided by 5.

[26]E. P. Chock, R. Chui, D. Davidov, R. Orbach, D. Shaltiel, and L. J. Tao, Phys. Rev. Lett. 27, 582 (1971).

[27]K. Baberschke and Y. v. Spalden, Phys. Rev. B 19, 5933 (1979).

[28]E. P. Chock, D. Davidov, R. Orbach, C. Rettori, and L. J. Tao, Phys. Rev. B 5, 2735 (1972).

[29]J. Nagel, K. Baberschke, and E. Tsang, J. Magn. Magn. Mater. 15-18, 730 (1980).

[30]R. Chui, R. Orbach, and B. L. Gehmann, Phys. Rev. B 2, 2298 (1970).

[31]D. Davidov, C. Rettori, A. Dixon, K. Baberschke, E. P. Chock, and R. Orbach, Phys. Rev. B 8, 3563 (1973).

[32]S. Oseroff, M. Passeggi, D. Wohlleben, and S. Schultz, Phys. Rev. B 15, 1283 (1977).